Chem Soc Rev

TUTORIAL REVIEW

View Article Online
View Journal

Cite this: DOI: 10.1039/d5cs01154j

Enantioselective reductive couplings and related transformations under cooperative photoredox catalysis

Yongjia Shi[a] and Daoshan Yang *[ab]

Received 28th September 2025

DOI: 10.1039/d5cs01154j

rsc.li/chem-soc-rev

The development of catalytic and enantioselective methods for constructing chiral carbon–carbon bonds remains a significant challenge and crucial objective in organic synthesis, as these chiral bonds are ubiquitous in bioactive molecules and natural products. The straightforward construction of chiral C–C bonds through asymmetric reductive coupling of two electrophiles represents one of the most powerful synthetic strategies in modern organic chemistry. Recently, photoredox catalysis has gained considerable attention from the scientific community due to its unique activation mode and significance for sustainable synthesis. The synergistic combination of photoredox catalysis and asymmetric catalysis has emerged as a promising catalytic strategy, offering a potential solution to overcome limitations in traditional asymmetric catalysis. This tutorial review offers a comprehensive overview of enantioselective reductive transformations under cooperative photoredox catalysis, focusing primarily on the synergistic interactions between photocatalysts and transition metals, enzymes, and hydrogen-bonding catalysts, highlighting their significance in understanding and advancing catalytic processes.

Key learning points

1. The background and key advantages of enantioselective reductive transformations.
2. The synergistic interaction patterns between photocatalysts and transition metals, enzymes, and hydrogen-bonding catalysts.
3. The modern methods for chiral C–C bond formation.
4. The role of photoredox catalysis and the associated mechanism.
5. The perspectives of future development in this field.

1 Introduction

Asymmetric catalysis lies at the cutting edge of modern chemistry and serves as a cornerstone for the highly selective synthesis of enantiomerically pure chiral molecules, which are essential in agrochemicals, pharmaceuticals, diagnostics, and advanced materials.[1] The development in recent decades has demonstrated that both chemical catalysis and biocatalysis have played pivotal roles, with approaches such as transition metal catalysis, hydrogen-bond catalysis, and enzyme catalysis emerging as powerful strategies.

1.1 Transition metal catalysis

Transition metals (TMs) have attracted widespread attention due to their distinctive reactivity and versatile catalytic modes. A large proportion of reported strategies for achieving the desired transformation have relied on adjusting either the ligand field or the oxidation state of the metal (Scheme 1a). The introduction of chirality has traditionally relied on the coordination of metal centers with one or more chiral ligands. Seminal contributions by Sharpless,[2] Knowles,[3] Kagan,[4] Noyori,[5] and others[6] led to the development of structurally diverse and highly efficient ligand architectures, including BINAP, TADDOL, JosiPhos, PHOX, Salen, DuPhos, BiOX, and PyBOX, among many others. These ligands, often referred to as ''privileged chiral ligands'', exhibit exceptional versatility, enabling a broad range of asymmetric transformations, such as cyclization,[7] cross-coupling,[8] hydrogenation,[9] oxidation,[10] and C–H bond activation.[11] Consequently, for over half a century,

[a] Key Laboratory of Optic-electric Sensing and Analytical Chemistry for Life Science, MOE, College of Chemistry and Molecular Engineering, Qingdao University of Science and Technology, Qingdao, 266042, P. R. China.
E-mail: yangdaoshan@tsinghua.org.cn
[b] National Engineering Research Center of Low-Carbon Processing and Utilization of Forest Biomass, Nanjing Forestry University, Nanjing 210037, China

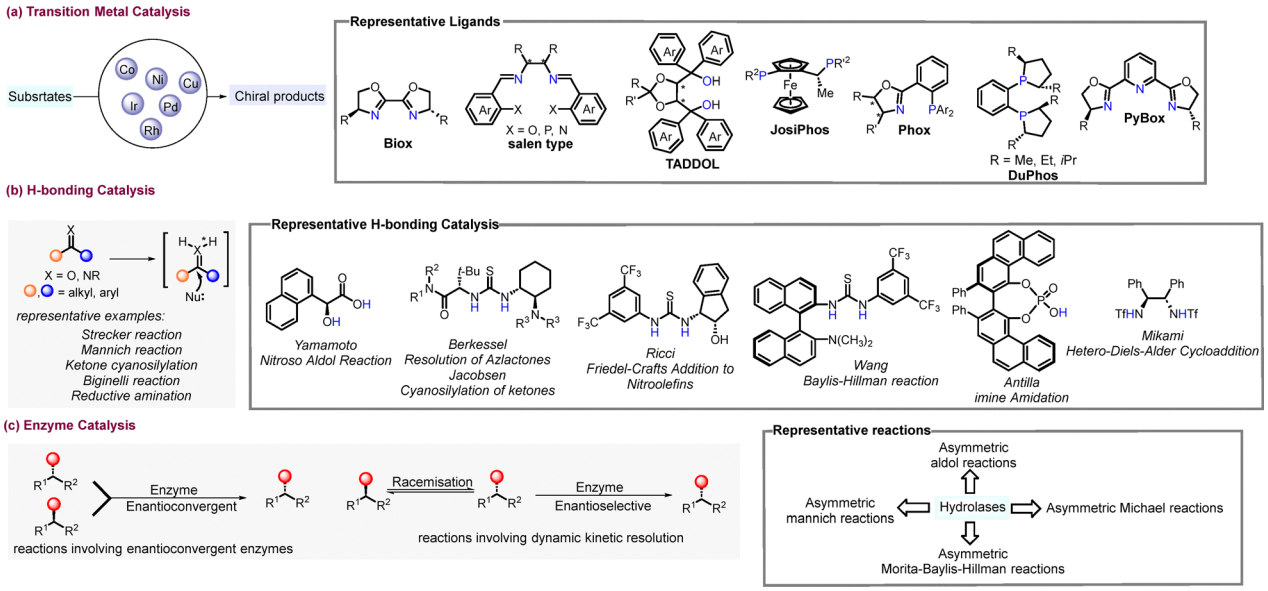

Scheme 1 (a) Transition-metal catalysis. (b) Hydrogen-bonding catalysis. (c) Enzyme catalysis for asymmetric transformations.

the design of chiral ligands has been remarkably successful and remains central to asymmetric transition-metal catalysis.

1.2 Hydrogen-bond catalysis

Chiral H-bonding catalysts primarily function by engaging in non-covalent interactions between the catalyst and substrates bearing oxygen- or nitrogen-containing functional groups as H-bond acceptors, and/or protons as donors. These directional H bonds not only facilitate the desired chemical transformations but also create a chiral environment conducive to the formation of stereogenic centers. To date, a wide variety of hydrogen-bonding catalysts with diverse structural and functional frameworks have been developed (Scheme 1b).[12] However, due to the relatively low binding energies associated with hydrogen bonding, such systems often require highly reactive substrates to achieve sufficient activation. This intrinsic limitation can restrict the substrate scope and confine the types of reactions amenable to this strategy.

1.3 Enzyme catalysis

Within biological systems, enzymes function as omnipresent natural catalysts, playing a crucial role in both natural biochemical processes and industrial applications.[13] According to Hult and Berglund, enzyme promiscuity can be broadly classified into three categories: (1) condition promiscuity, where the enzyme retains its activity under non-natural reaction conditions; (2) substrate promiscuity, where the enzyme can tolerate diverse substrates; and (3) catalytic promiscuity, where the

Yongjia Shi

Yongjia Shi was born in 1993 in Jinan, Shandong, P. R. China. She received her bachelor's degree in 2016 from Qufu Normal University. In 2021, she obtained her PhD degree from the Lanzhou Institute of Chemical Physics, Chinese Academy of Sciences, under the supervision of Prof. Senmiao Xu. She then joined the Lanzhou Institute of Chemical Physics as a research assistant. In 2024, she became an associate professor at the Qingdao University of Science and Technology. Her current research interests are focused on transition-metal catalysis, radical chemistry, photochemistry, and asymmetric catalysis.

Daoshan Yang

Daoshan Yang receive his PhD degree from Tsinghua University under the supervision of Prof. Hua Fu in 2012. Subsequently, he began his career at Qufu Normal University (2012–2020). Later, he joined Prof. Weiping Tang's group as a visiting scholar at the University of Wisconsin-Madison (2016–2017). From 2018 to 2019, he was a visiting professor at Fudan University under the guidance of Prof. Zhang-Jie Shi. Since 2020, he has been working as a full professor at Qingdao University of Science and Technology. His research interests include radical chemistry, photoredox catalysis, sulfur chemistry, and asymmetric catalysis.

enzyme's active site is capable of catalyzing more than one type of chemical transformation.[14] Enzymatic catalysis enables efficient and often reversible transformations under mild, environmentally benign conditions, such as asymmetric aldol reactions, Michael addition, Diels–Alder reactions, Knoevenagel condensation, Henry reaction, Mannich reaction, and Morita–Baylis–Hillman (MBH) reaction, among others (Scheme 1c).[15] However, the intricate three-dimensional structures that confer remarkable selectivity to enzymes also make them structurally fragile, which limits their broader application in synthetic chemistry.

1.4 Photoredox catalysis

Beyond traditional ionic reactions, radical-based transformations have gained widespread applications in synthetic chemistry due to their ability to enable unconventional bond cleavages and formations under mild conditions.[16] This versatility is driven by diverse radical generation strategies and the high intrinsic reactivity of radical species, as exemplified by photoredox catalysis, which employs photons as traceless and sustainable redox agents to generate reactive intermediates in both oxidative and reductive processes.[17] In this catalysis mode, the photosensitizer (**PC**) generates photoexcited species (**PC***) after absorbing visible light, which can function as both a 1e-oxidant and a 1e-reductant. Their redox potentials are structure-dependent and play a crucial role in the efficient generation of organic radicals. As depicted in Scheme 2, in a reductive quenching cycle, the excited state species (**PC***) can be reduced by electron donors (**D**) to afford the intermediates $\mathbf{PC}^{\bullet-}$ and $\mathbf{D}^{\bullet+}$. Generally, the $\mathbf{PC}^{\bullet-}$ species can react with the electron-deficient substrate **A** to generate the more reactive radical anion $\mathbf{A}^{\bullet-}$ with simultaneous regeneration of **PC**. Furthermore, in an oxidative quenching pathway, the excited-state **PC*** is oxidized by an electron acceptor **A** *via* single-electron transfer, affording a radical anion $\mathbf{A}^{\bullet-}$ and the oxidized form $\mathbf{PC}^{\bullet+}$, which can abstract an electron from electron-rich substrate **D**, thereby regenerating the ground-state PC. Both of the aforementioned species $\mathbf{D}^{\bullet+}$ and $\mathbf{A}^{\bullet-}$ can further participate in downstream transformations to generate the desired products.

Reductive cross-coupling (RCC) reactions have emerged as some of the most efficient strategies for constructing C–C and C–heteroatom bonds,[18] due to their ability to couple two readily available and structurally robust electrophiles, thereby circumventing the need for prefunctionalized, stoichiometric organometallic reagents that are often highly sensitive to air and moisture. Unlike traditional cross-coupling approaches that rely on nucleophilic partners, RCC reactions leverage inexpensive halides, pseudohalides, or other electrophilic building blocks as coupling partners, which are typically more stable, cost-effective, and widely accessible. The inherent redox-neutral or mild reductive conditions employed in these reactions enable high functional group tolerance, enabling RCC particularly attractive for complex molecule synthesis and late-stage functionalization.

Although Kuhn began investigating enantioselective photochemical reactions as early as the 1930s,[19] achieving enantioselectivity solely through chiral photoredox catalysts under visible-light irradiation remains rare. To date, Meggers,[20] Yoon,[21] and others[22] have developed a series of chiral photoredox catalysts, including inorganic chromophores, soluble macromolecules and chiral organic sensitizers.[23] Nevertheless, they are relatively limited, and are typically not used for reductive cross-coupling. Moreover, photoredox catalysis alone is often insufficient to facilitate selective cross-coupling reactions, as single-electron transfer (SET) processes typically activate only one of the two electrophilic partners, leaving the other unreactive. In addition, SET mechanisms inherently lack spatial control, presenting a significant challenge for the establishment of well-defined coordination environments. To overcome these limitations, dual catalytic strategies have garnered growing attention.[24–30] In such cooperative systems, various transition-metal complexes and organic dyes, due to their highly adjustable redox potentials, can serve as photocatalysts to generate reactive radical intermediates (Scheme 3a), which are subsequently intercepted by a second catalyst that promotes bond formation with the second electrophile in a stereocontrolled fashion. These dual catalytic platforms not only broaden substrate scope but also enhance reactivity, selectivity, and functional group tolerance.[31]

Although significant progress has been made in the field of photo-induced asymmetric catalysis, asymmetric reductive transformations with light intervention is still in its infancy. Although several excellent review articles have been published

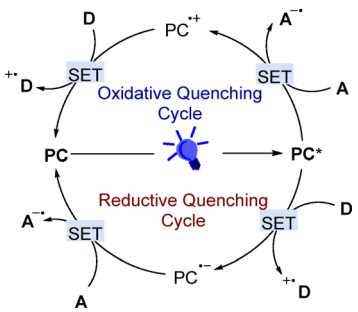

Scheme 2 The mechanism of light-driven photoredox catalysis.

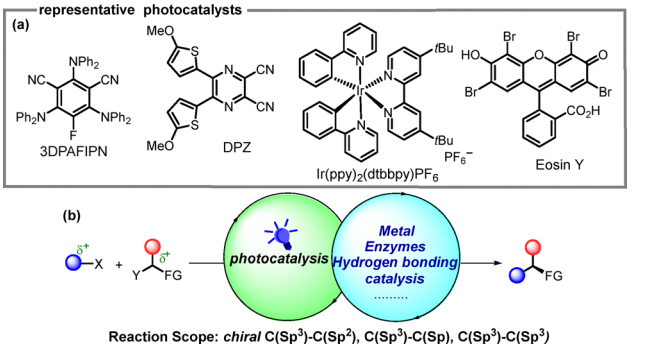

Scheme 3 (a) Representative photocatalysts. (b) Enantioselective reductive transformations under cooperative photoredox catalysis.

in this field,[32] they predominantly focused on a specific aspect. To date, no comprehensive tutorial review on photocatalytic asymmetric reductive transformations has been published. In this guiding review, we will discuss the advancements of the progress of visible light-promoted enantioselective reductive cross-coupling between two electrophiles and related transformations in dual catalytic systems, mainly including the synergistic effects of visible light with transition metals, hydrogen bonding catalysts, and enzymes (Scheme 3b).

2 Cooperative photoredox and transition-metal dual catalysis

2.1 Nickel/photoredox cooperative catalysis

Nickel (Ni) features comparatively low electronegativity and negative reduction potentials, allowing it to reversibly access multiple oxidation states (Ni^0, Ni^I, Ni^{II}, and Ni^{III}) under mild conditions,[33] which renders it particularly well suited for efficient integration with photoredox catalytic cycles *via* single-electron transfer (SET) processes.[34] In cooperative photoredox systems, this manifold of accessible oxidation states enables Ni to play two key roles: on the one hand, it reacts with electrophiles such as aryl, alkenyl, alkynyl, or alkyl halides to form Ni–C intermediates; on the other hand, it efficiently captures carbon-centered radicals generated in the photoredox cycle and forges new C–C bonds through stereoselective reductive elimination from high-valent Ni species.[35] Consequently, dual Ni/photoredox catalysis has emerged as a central platform for the construction of chiral $C(sp^3)$–$C(sp^2)$, $C(sp^3)$–C(sp), and even $C(sp^3)$–$C(sp^3)$ bonds, as well as for enabling selected difunctionalization transformations.[36] In particular, nickel is particularly powerful in cross-electrophile couplings that combine (hetero)aryl or alkenyl halides with alkyl partners, where its ability to perform both oxidative addition to $C(sp^2)$ electrophiles and rapid capture of alkyl radicals distinguishes it from other metals.

2.1.1 Chiral C_{sp^3}–C_{sp^2} bond formation. In cross-electrophile coupling, the primary challenge is to achieve selective cross-coupling between two different electrophiles rather than undesired homocoupling (Scheme 4a).[37] Building on the general features outlined above, nickel-catalyzed reactions proceeding *via* a radical chain process generally comprises five elementary steps: oxidative addition, radical addition, reductive elimination, radical generation, and reduction (Scheme 4b). In 2013, to determine whether the aryl or alkyl Ni(II) intermediate was formed at the initial stage, Biswas *et al.* conducted a preferential competition experiment of the RCC between iodobenzene **1** and iodooctadecane **2** catalyzed by Ni^0/**L1** (**L1** = 4,4′-di-*tert*-butyl-2,2′-bipyridine, dtbpy) (Scheme 4c).[38] The results revealed that iodobenzene undergoes oxidative addition to the Ni^0 species 4.7 times faster than iodooctadecane, indicating that the aryl–Ni(II) intermediate is formed preferentially during the reaction. This can be attributed to the favorable π–metal interaction between the metal center and the substrate.[39] Multiple

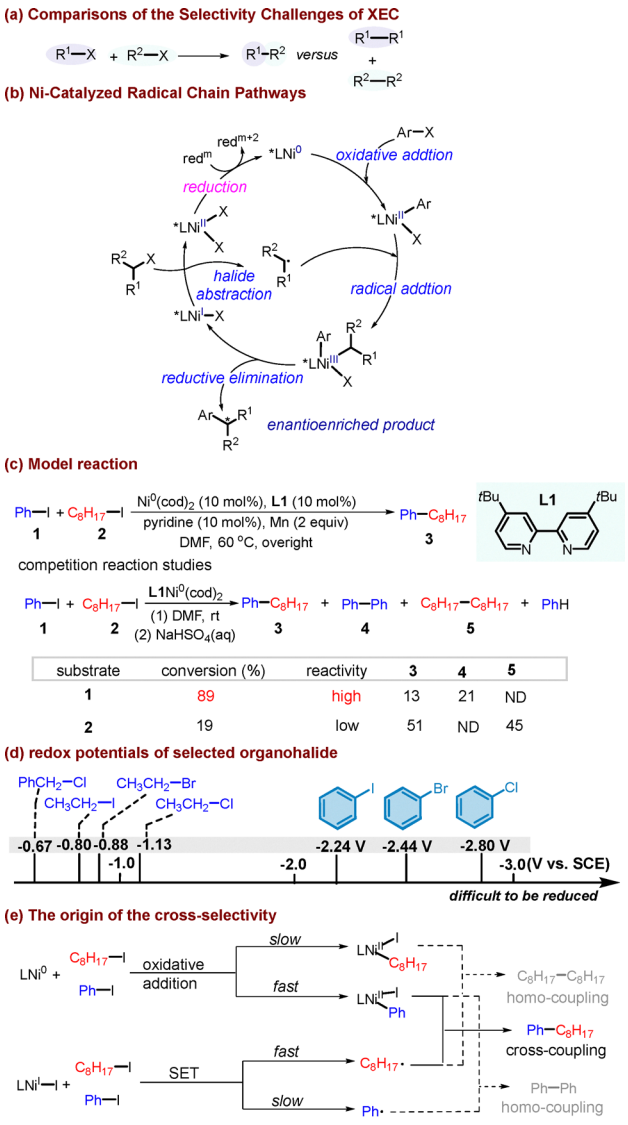

Scheme 4 (a) Comparisons of the selectivity challenges of cross-electrophile coupling (XEC). (b) Ni-catalyzed radical chain pathways. (c) Model reaction and competition studies. (d) Redox potentials of selected organohalides. (e) The origin of cross-selectivity.

theoretical studies have confirmed that the oxidative addition (OA) rate of $C(sp^2)$ electrophiles is faster than that of $C(sp^3)$ electrophiles. For example, Ren and co-workers found that the activation barrier for aryl halides is 4.4 kcal mol^{-1} lower than that for alkyl halides.[40] Consistent findings were independently reported by Kumar *et al.*[41] In addition, the distinct reduction potentials of $C(sp^2)$ and $C(sp^3)$ electrophiles result in $C(sp^3)$ electrophiles being more efficiently engaged through radical-mediated activation pathways (Scheme 4d).[42] Therefore, the mechanism begins with oxidative addition to form a Ni(II)–aryl intermediate, which preferentially reacts with $C_8H_{17}I$ over PhI, leading to the generation of an alkyl radical. This sequential activation pathway accounts for the cross-selectivity observed in the experiment (Scheme 4e).[38] More importantly, the use of an external electron donor is essential for accessing low-valent

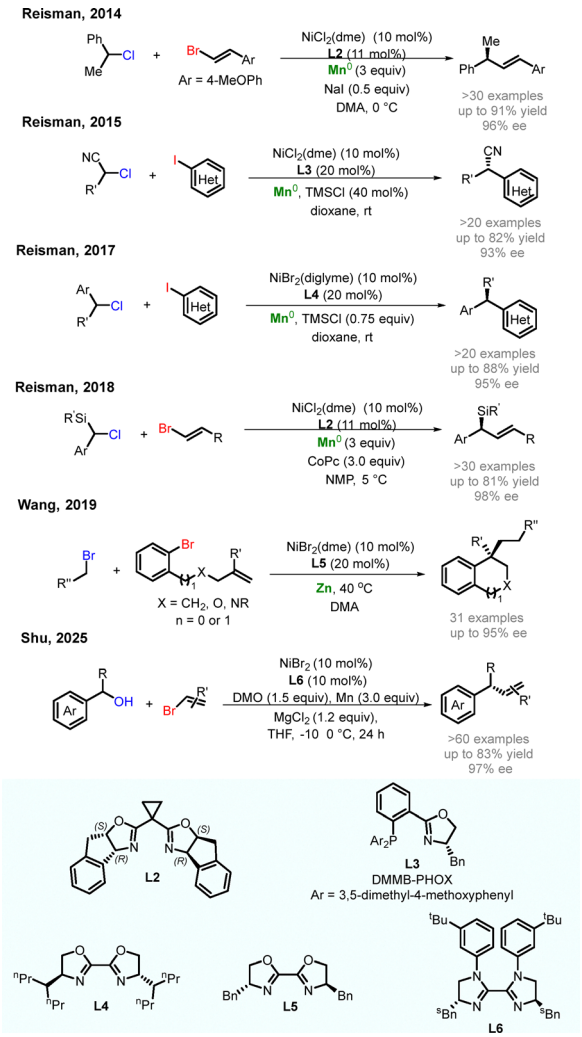

Scheme 5 Ni-Catalyzed enantioselective reductive cross-coupling.

nickel species, which are required for the activation of aryl and alkyl halides and for facilitating the redox cycling of nickel in selective C–C bond-forming processes.[43] More than a century ago, Wurtz, Tollens, and Fittig laid the groundwork for cross-electrophile coupling by employing sodium metal between aryl and alkyl halides.[44] These early methods required harsh conditions, including elevated temperatures and stoichiometric amounts of sodium as both a mediator and reductant. As a result, the utility of these reactions was significantly limited by poor functional group tolerance and narrow substrate scope. Subsequent advances employed inexpensive metal reductants such as zinc and manganese, offering improved practicality under milder conditions (Scheme 5).[45] However, the application of stoichiometric metallic reductants presents several limitations. Firstly, metal powders often require preactivation to expose reactive surfaces. Secondly, their reactivity may vary significantly depending on the quality or supplier of the metal source. Thirdly, certain functional groups are incompatible with reductive metals, potentially leading to undesired side reactions. Moreover, increasing emphasis has been placed on

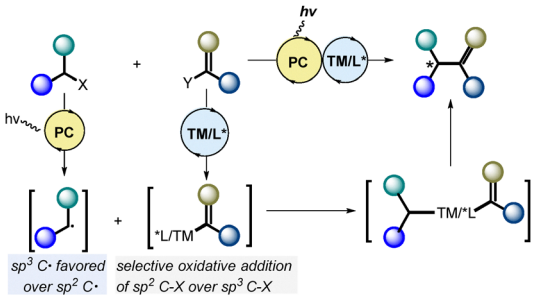

Scheme 6 Enantioselective metallaphotoredox catalysis.

the development of tunable reductive systems to enhance the generality and functional compatibility of RCC transformations. To address these challenges, organic reductants such as B_2pin_2 and hydrazine have been discovered. However, the scope of reactions that can be enabled by these reductants remains limited.[46] Nickel/photoredox catalysis offers a novel synthetic strategy, in which the core characteristics of the Ni-mediated catalytic cycle remain fundamentally consistent despite variations in the reduction conditions, primarily affecting the pathway of radical generation. For instance, electron donors such as tris(trimethylsilyl)silane,[47] amines,[48] and Hantzsch esters,[49] although their redox potentials do not align with the requirements for nickel reduction, have shown remarkable efficiency in selective reductive coupling under cooperative catalytic conditions, thereby significantly expanding the synthetic utility of these transformations (Scheme 6).

In 2020, Mao and co-workers reported a nickel-catalyzed reductive cross-coupling of aryl iodides with α-chloro esters under visible-light conditions employing an organic reducing agent Hantzsch ester 1,4-dihydropyridine (HEH) to afford α-aryl esters and their derivatives,[50] which can serve as precursors to non-steroidal *anti*-inflammatory agents (Scheme 7a).[51] Meanwhile, this reaction utilized 1,2,3,5-tetrakis (carbazol-9-yl)-4,6-dicyanobenzene (4CzIPN) as the photocatalyst, thus allowing both coupling partners to be engaged under mild conditions and avoiding the use of preformed unstable organometallic reagents. According to the mechanism, [Ni^0] species preferentially undergo oxidative addition with aryl iodides to produce [Ni^{II}] complex due to kinetic advantages. Subsequently, the α-chloro ester, benefiting from a more favorable reduction potential, is more prone to undergoing single-electron transfer (SET) to afford an α-carbonyl radical *via* three possible pathways, as shown in Scheme 8. The reduction may occur from [Ni^0], [Ni^I] or reduced photocatalyst 4CzIPN$^{\bullet-}$, which can be generated by the SET process between HEH and the photo-excited state photocatalyst 4CzIPN*. Next, the α-carbonyl radical is rapidly captured by the [Ni^{II}] complex to form the reactive [Ni^{III}] species, which is followed by rapid reductive elimination to afford the final product. In addition, the [Ni^0] species can be regenerated by SET with 4CzIPN$^{\bullet-}$, completing the whole catalytic cycle. Despite these advantages, these systems remain largely confined to aryl iodides and highly activated α-chloro carbonyl electrophiles. Electron-rich or sterically congested aryl

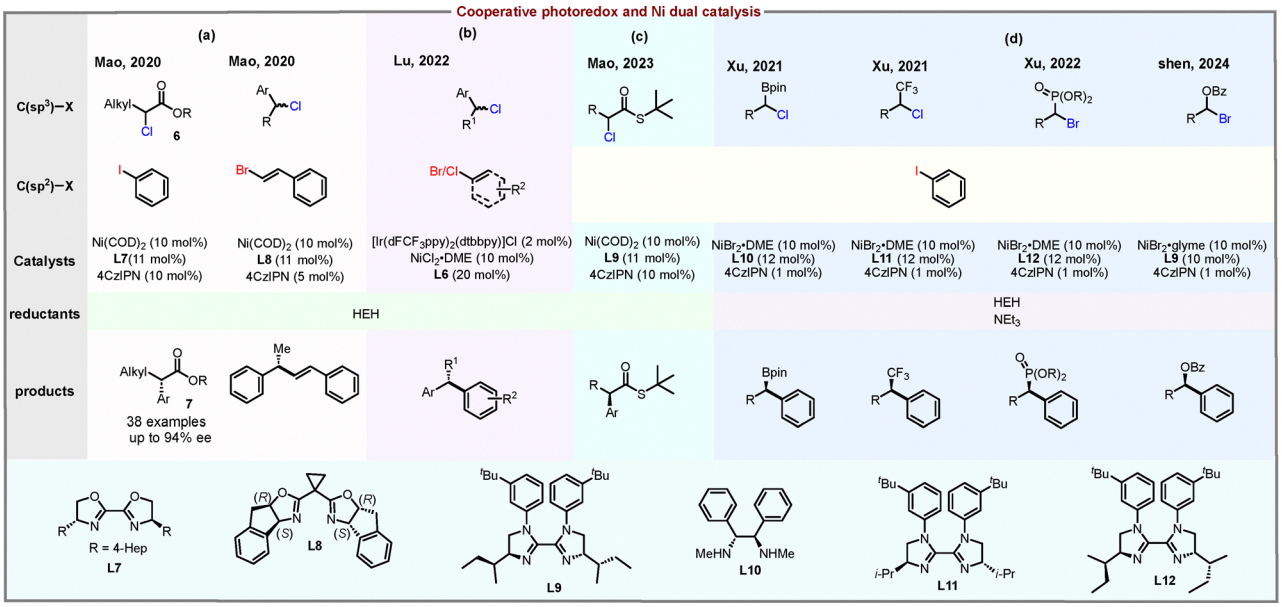

Scheme 7 Nickel/photoredox-catalyzed enantioselective reductive cross-coupling.

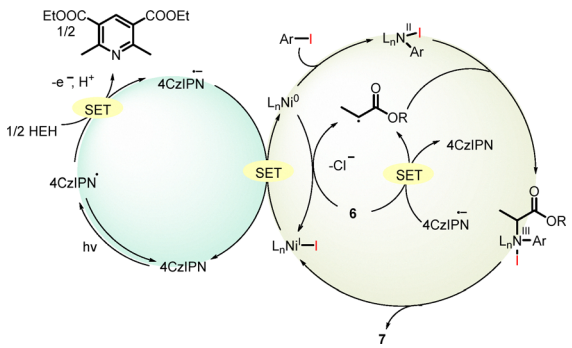

Scheme 8 Plausible catalytic reaction pathway for the Ni/photoredox-catalyzed reductive cross-coupling of aryl iodides with α-chloro esters.

partners typically deliver diminished yields. Subsequently, Lu and Mao further employed HEH to extend this system to the nickel/photoredox-catalyzed RCC of vinyl bromides and benzyl chlorides, as well as α-chlorothioesters with aryl iodides (Scheme 7b and c).[52]

Early mechanistic investigations indicated that the Hantzsch ester could exhibit enhanced reducing ability in the presence of triethylamine (Et_3N). In 2021, Xu and co-workers demonstrated a dual nickel/photoredox-catalyzed RCC of α-chloroboranes and aryl iodides to construct chiral benzylic boronic esters (Scheme 7d).[53] This process was carried out using photocatalyst 4CzIPN and a commercially available ligand **L10** under mild conditions (ambient temperature, visible light, and no strong bases) with Et_3N or HEH as the reducing agent, and it is compatible with a variety of functional groups. Regarding the mechanism, the photocatalyst 4CzIPN is excited to the photoexcited 4CzIPN* under visible light irradiation firstly, which is then reduced by Et_3N or HEH to $4CzIPN^{\bullet-}$.

It subsequently combines with the nickel cycle to provide the boron-stabilized radical **I**. On the other hand, [Ni^0] species can undergo oxidative addition with aryl iodide to produce [Ni^{II}] species, which is then oxidized by boron-stabilized radical **I** to form [Ni^{III}] intermediate. Next, reductive elimination of [Ni^{III}] intermediate generates the target product and [Ni^{I}] species. Finally, the [Ni^{I}] species is reduced by $4CzIPN^{\bullet-}$ to regenerate the [Ni^0] species and photocatalyst 4CzIPN, completing the catalytic cycle (Scheme 9). Afterward, they further achieved the RCC of CF_3-substituted racemic alkyl electrophiles or α-bromophosphates[49] and aryl halides,[54] providing access to synthetically useful chiral CF_3-containing compounds and

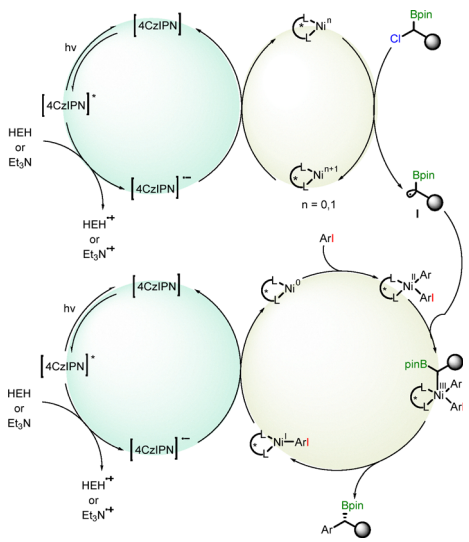

Scheme 9 Plausible catalytic pathway for the Ni/photoredox-catalyzed reductive cross-coupling of α-chloroboranes with aryl iodides.

α-aryl phosphorus. Moreover, in 2024, Shen and co-workers accomplished a nickel/photoredox-catalyzed asymmetric RCC of α-bromobenzoates with aryl halides (Scheme 7d).[55] This photochemical protocol employed the ligand **L9** and HEH or NEt_3 as the reductant to enable the synthesis of chiral benzyl alcohols derivatives. However, these systems are mainly restricted to combinations of aryl iodides with specific α-halogenated electrophiles, and typically deliver only moderate yields for substrates with more demanding electronic or steric profiles, indicating that their generality and expandability still require further improvement.

Beyond asymmetric reductive couplings between two halide partners, this strategy can also be extended to epoxides. Actually, due to their facile generation from alkenes and their susceptibility to nucleophilic attack, epoxides serve as important and broadly utilized platforms in modern organic synthesis.[56] Chiral catalyst-controlled asymmetric ring-opening of epoxides provides an effective strategy for asymmetric synthesis (Scheme 10a),[57] with substantial advances achieved using soft nucleophiles or heteroatom-based reagents such as water, azide, and cyanide.[58] Although catalytic C–C bond-forming processes employing organolithium or organomagnesium nucleophiles are known, these approaches generally require rigorous conditions and exhibit poor tolerance toward sensitive functionalities.[59] Moreover, the use of chiral epoxides often results in kinetic resolution, since their ring-opening reactions typically proceed in a stereospecific fashion. The first enantioselective cross-electrophile coupling of *meso*-epoxides was reported by Weix and co-workers, employing a chiral titanocene cocatalyst in concert with a racemic Ni catalyst (Scheme 10b).[60] Building on this progress, Yamamoto's group demonstrated the Ni-catalyzed arylation of 3,4-epoxyalcohols with chiral BiOx ligands, which provided cross-coupled products in outstanding levels of *enantio-* and diastereocontrol.[61] This transformation, however, requires a pendant hydroxyl group within the epoxide substrate to achieve effective stereochemical induction. While these contributions represent significant milestones, the development of complementary methods, particularly those that enable stereoconvergent coupling of racemic terminal epoxides, remains an important goal to broaden the utility of this strategy. In 2021, Doyle *et al.* developed a nickel/photoredox-catalyzed enantioselective cross-electrophile coupling (XECs) of aryl iodides with epoxides, enabling a direct approach to chiral 2,2-diaryl alcohols with moderate yields and high enantioselectivities (Scheme 10c).[62] This catalytic system can be established using 4CzIPN as a photocatalyst, chiral biimidazoline (BiIm) **L11** as a ligand and NEt_3 as a reducing agent. Nonetheless, the current system is largely restricted to styrene oxides and aryl iodides, aliphatic epoxides and more electron-deficient aryl coupling partners generally perform poorly. Mechanistic experiments and computations indicate that reductive elimination is enantiodetermining and that ligand electronics modulate enantioselectivity by shifting the transition-state structure along the reaction coordinate. A $[Ni^0]/[Ni^{II}]/[Ni^{III}]/[Ni^{I}]$ catalytic cycle featuring a halohydrin intermediate was proposed. Firstly, the

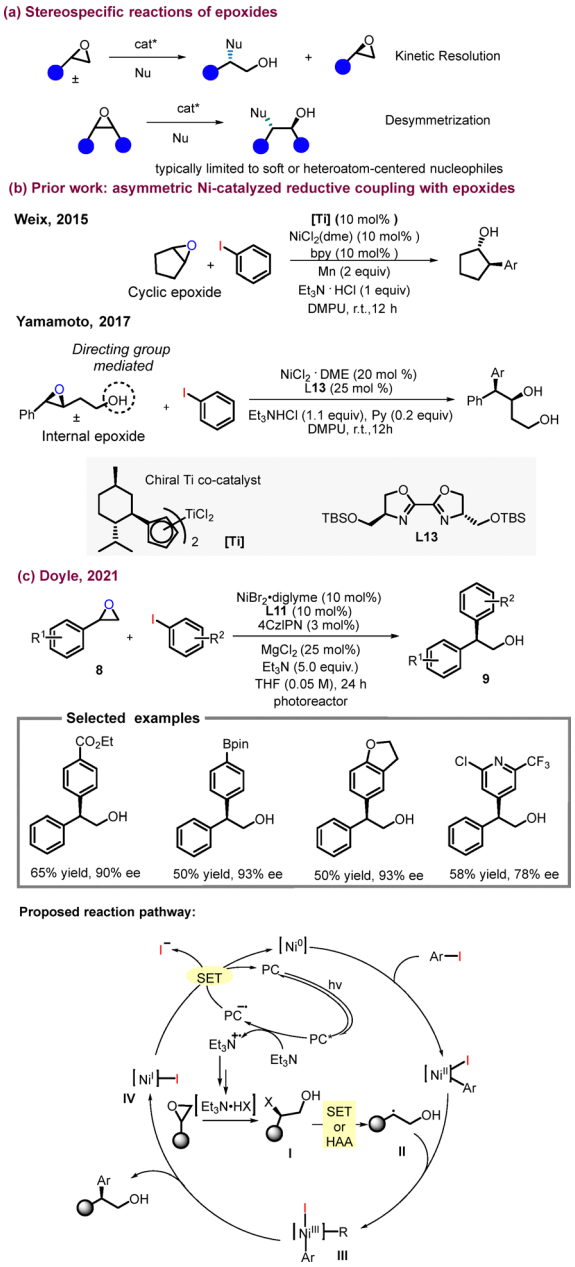

Scheme 10 Strategies for asymmetric synthesis with epoxides and nickel/photoredox-catalyzed asymmetric cross-coupling of styrene oxides and aryl iodides.

oxidative addition of $[Ni^0]$ species with aryl iodide give $[Ni^{II}]$ species. Meanwhile, the *in situ* formed HX (X = Cl, Br, I) nucleophilically opens the ring of racemic epoxide **8** to yield the halohydrin intermediate **I**, which may proceed *via* a SET process or halogen atom extraction to produce the secondary radical **II**. Next, the radical is trapped by the $[Ni^{II}]$ complex to produce $[Ni^{III}]$ species **III**, followed by reductive elimination to give the target product **9** and $[Ni^{I}]$ species **IV**. Furthermore, reductive quenching to the excited state of 4CzIPN by triethylamine yields $4CzIPN^{\bullet -}$, which can reduce $[Ni^{I}]$ species **IV** to an $[Ni^0]$ complex, completing the catalytic cycle.

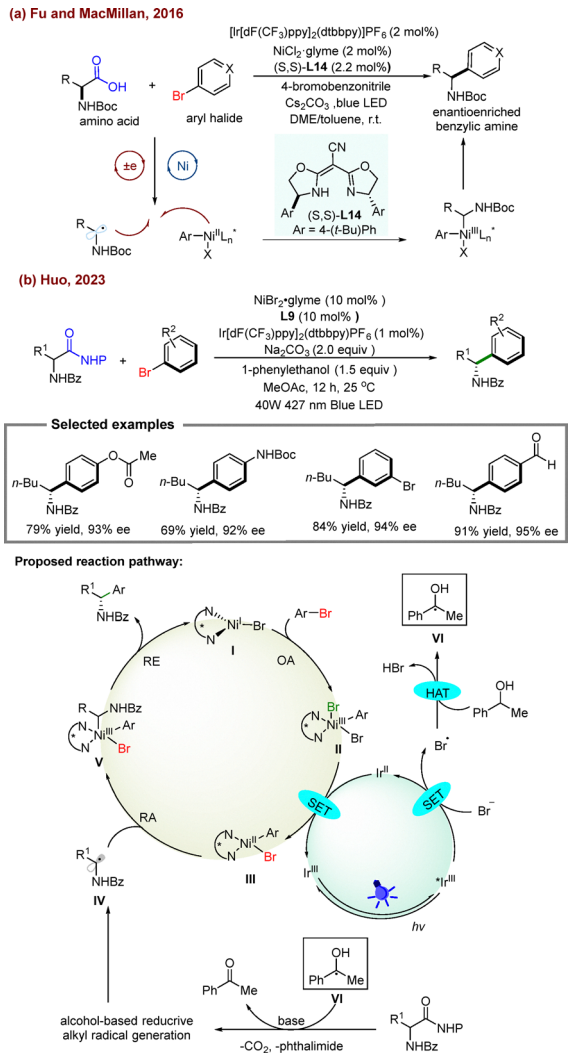

Scheme 11 Nickel/photoredox-catalyzed asymmetric reductive coupling of α-amino acid–derived radical precursors.

Beyond amines, inexpensive, abundant, and tunable alcohols can also be applied as reducing agents to achieve chiral-selective XECs. In 2023, Huo and co-workers demonstrated a Ni/photoredox-catalyzed enantioselective XEC of (hetero)aryl bromides and α-amino acid derivatives *via* a halogen radical-mediated HAT process employing a readily available benzyl alcohol as the reducing agent to afford various benzylic amines in high yields and with excellent enantioselectivities (Scheme 11b).[63] Although metallaphotoredox decarboxylative arylation has been applied to a range of substrates, several challenges still remain, including (i) sluggish oxidative addition, (ii) limited asymmetric induction, and (iii) sensitivity to coordinating functional groups.[64] A notable advance from the Fu and MacMillan labs introduced a mechanistically distinct decarboxylative asymmetric arylation *via* oxidative activation of α-amino acids (Scheme 11a).[65] Nevertheless, this approach is largely confined to electron-deficient aryl bromides. By comparison, this strategy accommodates more demanding electron-neutral and electron-rich (hetero)aryl bromides and enables late-stage functionalization while tolerating a variety of functional groups. However, the current protocol is mainly restricted to NHP esters derived from α-amino acids and relies on a specific benzylic alcohol reductant under basic conditions; its performance with more complex peptide-like substrates or other carboxylic acid derivatives has not yet been fully explored. A depicted mechanism for this transformation is provided. Initially, the photocatalyst is excited to an excited state under light irradiation, which can then oxidize the bromine anion to generate a bromine radical. Subsequently, it undergoes a HAT process with 1-phenylethanol to form an α-hydroxyalkyl radical **VI**. Under base-containing conditions, NHP esters and the resulting radical **VI** can generate an α-amino carbon-centered radical **IV** and acetophenone by a SET or proton-coupled electron transfer (PCET) process. In addition, aryl bromide reacted with [Ni^{I}] complex **I** to give [Ni^{III}] complex **II** by oxidative addition, which could be reduced by the reduced photocatalyst to afford [Ni^{II}] complex **III**, while it could easily intercept α-amino radical **IV** to give [Ni^{III}] complex **V**, which could then undergo the reduction and elimination process to produce the target product and [Ni^{I}] complex **I**, completing the catalytic cycle.

The direct reductive cross-coupling of alkyl alcohols with aryl halides remains challenging due to the high bond dissociation energy of the C–O bond and the poor leaving ability of the hydroxyl group.[66] To address this limitation, various alcohol derivatives including xanthate esters,[67] alkyl acetates,[68] pivalates,[69] mesylates,[70] oxalates,[71] chloroformates,[72] tosylates,[73] methyl ethers,[74] and others[75] have been explored in reductive cross-coupling reactions. Most of these strategies are restricted to activated alcohol derivatives and require additional pre-activation steps. In 2018, Ukaji and co-workers reported a titanium-mediated direct reductive cross-coupling, which is limited to primary benzyl alcohols.[76] Alternatively, one-pot procedures combining *in situ* alcohol activation with subsequent reductive cross-coupling have shown promise. Pioneering studies by Gong,[77] Shu,[78] Weix,[79] Li,[80] and others[81] demonstrated the potential of this approach by utilizing the broad availability of free alcohols and aryl bromides. A notable breakthrough was achieved by the MacMillan group in 2021, who developed an N-heterocyclic carbene enabled deoxygenative arylation (Scheme 12a).[82] This method operates under mild conditions, is operationally simple, and is compatible with a broad range of primary, secondary, and tertiary alcohols. Nevertheless, the development of enantioconvergent deoxygenative reductive cross-coupling, particularly for unactivated alkyl alcohols, remains a huge challenge. In 2024, Yang and co-workers described a nickel/photoredox-catalyzed enantioselective deoxygenative reductive cross-coupling of aryl bromines and unactivated alkyl alcohols to afford various β-aryl ketones under visible-light irradiation in the presence of an NHC activating agent (Scheme 12b).[83] In this system, a series of substituents on ketones are tolerated, including silyl ether, boc-protected amine, ether, ester, thiophene, furan, *etc.*, which give products with good yields and excellent enantiomeric excesses. Furthermore, aryl bromines containing electron-rich or electron-

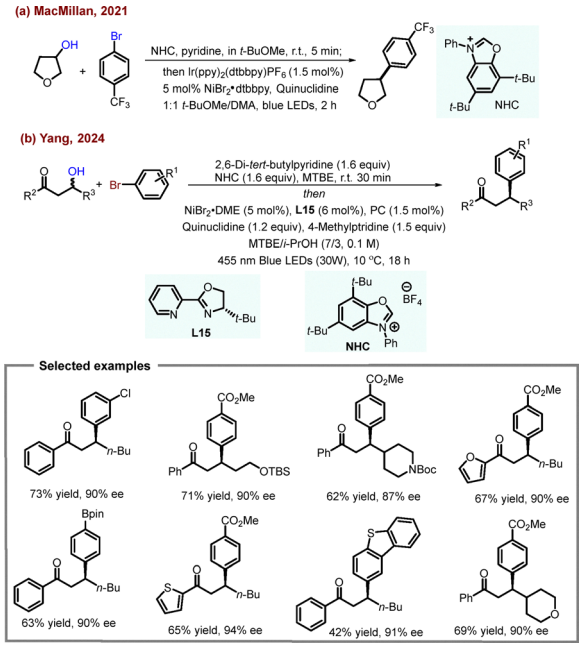

Scheme 12 Nickel/photoredox-catalyzed enantioselective deoxygenative reductive cross-coupling.

deficient substituents such as Bpin, trifluoromethyl, benzothiophene, benzofuran and others participate efficiently to yield the target products in good yields. At the same time, the current protocol relies on *in situ* activation with a stoichiometric NHC reagent and has so far been demonstrated mainly for β-aryl ketones derived from relatively simple aryl bromides and monohydric alcohols. Applications to more complex polyols, strongly coordinating or base-sensitive functional groups, and other classes of electrophiles have not yet been demonstrated, highlighting the need for further work to generalize this enantioconvergent deoxygenative coupling manifold.

2.1.2 Chiral C_{sp^3}–C_{sp} bond formation. Optically active organophosphonates, which can be broadly employed in the fields of agrochemicals, pharmaceuticals and asymmetric catalysis chemistry, and their synthesis has garnered significant attention.[84] In 2023, Xu *et al.* realized a nickel/photoredox catalyzed enantioselective C(sp)–C(sp^3) reductive cross-coupling of α-bromo phosphonates and alkynyl bromides using the strategy of halogen atom transfer (Scheme 13a).[85] It is worth mentioning that chiral α-alkynyl phosphonates can be constructed using $NiBr_2$(DME) and 3DPAFIPN as the dual catalysts, bidentate nitrogen ligand **L16** as the chiral ligand, Cy_2NMe as the reductant, and K_2CO_3 as the base. Under these conditions, a range of α-bromo phosphonates and alkynyl bromides are converted to the desired products in generally good yields and high enantioselectivities. In these studies, the halide electrophiles are readily accessible and enable the modular assembly of different phosphonate-containing scaffolds. However, current variants are mainly limited to α-bromo phosphonates and alkynyl bromides bearing relatively simple aryl or alkyl substituents, and rely on superstoichiometric Cy_2NMe under

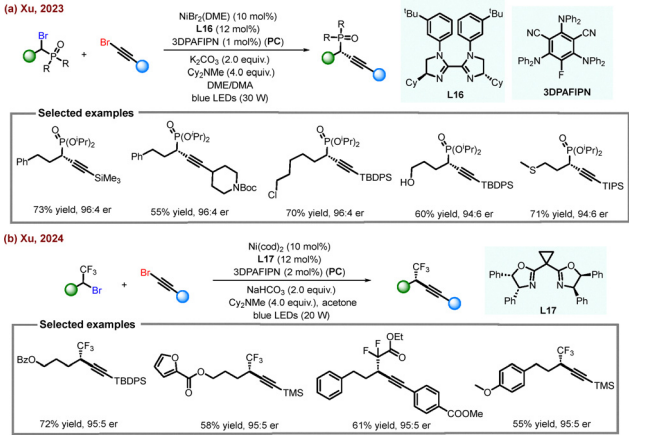

Scheme 13 Nickel/photoredox catalyzed enantioselective C(sp)–C(sp^3) reductive coupling.

basic conditions. Considering a trifluoromethyl (CF_3) group usually significantly improves the physicochemical and biological properties of the molecule, such as its lipophilicity, bioavailability and metabolic stability,[86] and the same group further expanded the system to the efficient construction of chiral trifluoromethylated alkynes (Scheme 13b).[87] Future studies that expand this manifold to more complex architectures, other C(sp) electrophiles, and densely functionalized or strongly coordinating substrates would be highly desirable.

2.1.3 Chiral C_{sp^3}–C_{sp^3} bond formation. In 2024, Xu and co-workers developed a dual nickel/photoredox catalyzed enantioselective reductive cross-coupling of alkyl iodides and racemic α-chloroboronates, leading to the chiral α,α-dialkyl boronic esters (Scheme 14).[88] Using 4CzIPN as the photocatalyst, (*S*,*S*)-L18 as the ligand, HEH as the reducing agent, and $NaHCO_3$ as the base, chiral secondary alkyl boronic esters are obtained in high yields with excellent chemo- and stereoselectivities. Sulfonamide, ester, ether, thiophene, protected indole, alkyl chloride, alkene and other functional groups are tolerated under the standard conditions. The reaction begins with the oxidative addition of α-chloroboronate to the (L18)Ni(I) complex I, affording a Ni(III) intermediate II. Subsequent photoredox-mediated reduction furnishes the (L18)Ni(II) species III, which is then oxidized by the alkyl radical generated from the corresponding alkyl iodide to deliver intermediate IV. This species participates in enantioselective C–C bond formation and simultaneously regenerates the (L18)Ni(I) catalyst I, thereby completing the catalytic cycle. Despite the high levels of chemo- and enantioselectivity, the current protocol is mainly limited to α-chloroboronates and simple primary or secondary alkyl iodides, and relies on superstoichiometric HEH under mildly basic conditions. More sterically congested or strongly coordinating substrates, as well as other classes of boron electrophiles or radical precursors, have not yet been shown to be compatible.

2.1.4 Reductive dicarbofunctionalization for chiral C–C bond formation. In 2021, Mao and co-workers disclosed a nickel/photoredox-catalyzed three-component alkyl arylation

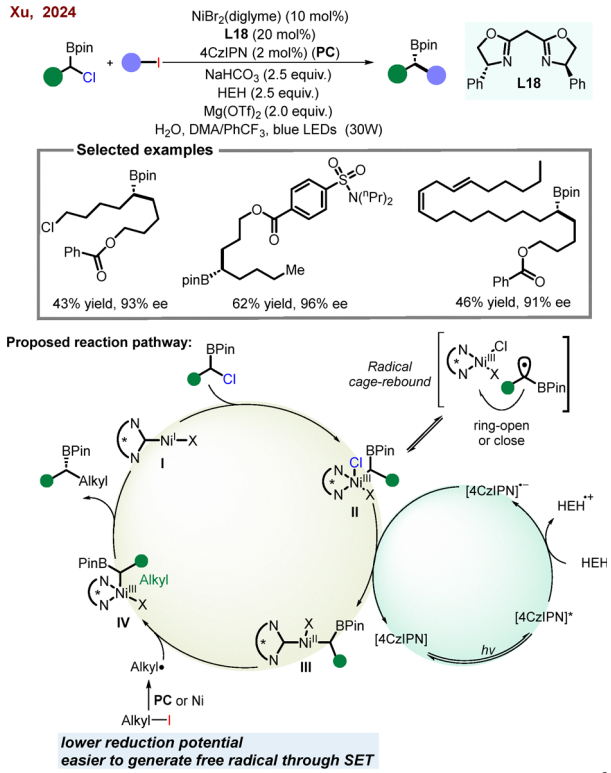

Scheme 14 Nickel/photoredox-catalyzed enantioselective C(sp^3)–C(sp^3) reductive cross-coupling of alkyl iodides and racemic α-chloroboronates.

of acrylates to afford chiral α-aryl propionic acids that constitute an important class of nonsteroidal anti-inflammatory drug derivatives (NSAIDs) (Scheme 15).[89] This method employed two electrophiles that are commercially available and can participate under relatively mild conditions. Mechanistically, in the presence of visible light, 4CzIPN is excited to 4CzIPN*, which can be reduced by HEH or Cy_2NMe to produce the anionic radical $4CzIPN^{\bullet-}$ firstly. $(Ln)Ni^{II}$ complex **I** then reacts with the reduced photocatalyst $4CzIPN^{\bullet-}$ to give the $(Ln)Ni^{0}$ complex **II** *via* a two SET process. Subsequently, oxidative addition of the resulting $(Ln)Ni^{0}$ complex **II** with aryl bromide gives the (Ln)Ni(Ar)Br complex **III**. Alternatively, alkyl bromide can react with $(Ln)Ni^{0}$ complex **II** or reduced photocatalyst $4CzIPN^{\bullet-}$ *via* a SET process to form alkyl halide anion, releasing bromine to produce the tertiary radical, which can be added to acrylate to generate the α-carbonyl radical **IV**. Next, the radical **IV** is captured by the $(Ln)Ni^{II}$ complex **III** to generate the Ni^{III} intermediate **V**, which undergoes a reductive elimination process to generate the target product. Despite the high levels of regio- and enantioselectivity, this protocol is mainly demonstrated for acrylate-type Michael acceptors in combination with tertiary alkyl bromides and aryl bromides; extension to less activated alkenes, primary or secondary alkyl electrophiles, and more strongly coordinating functional groups remains limited, and superstoichiometric organic reductants are still required.

In 2024, Chu and co-workers reported a nickel/photoredox-catalyzed asymmetric three-component XEC of vinyl boronates,

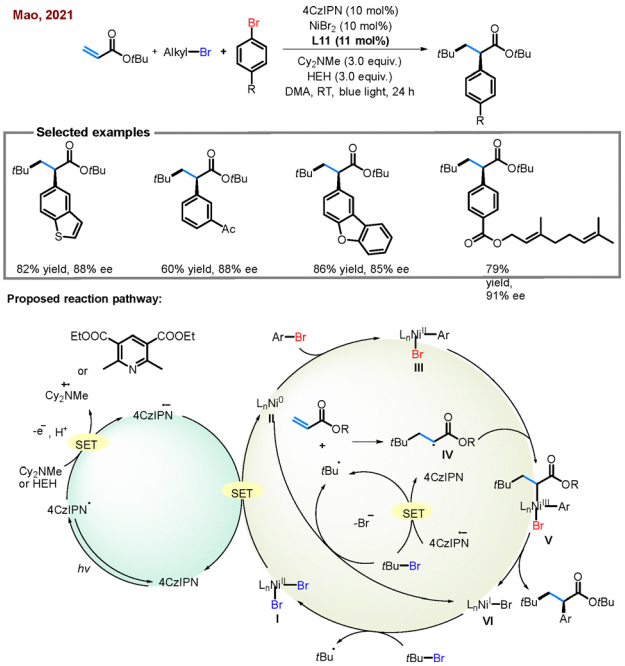

Scheme 15 Nickel/photoredox-catalyzed three-component alkyl arylation of acrylates.

(hetero) aryl bromine and (2°, 3°) alkyl redox-activated esters (Scheme 16).[90] This method provides access to chiral β-alkyl-α-arylboronic esters with excellent regioselectivities and enantioselectivities employing the newly developed chiral biimidazoline ligand **L19** under mild conditions. Nevertheless, the current system is largely confined to vinyl boronate partners and (hetero)aryl bromides, relies on redox-active esters derived from relatively simple secondary and tertiary alcohol or amine precursors, and has not yet been broadly validated for densely functionalized or strongly coordinating substrates. Further

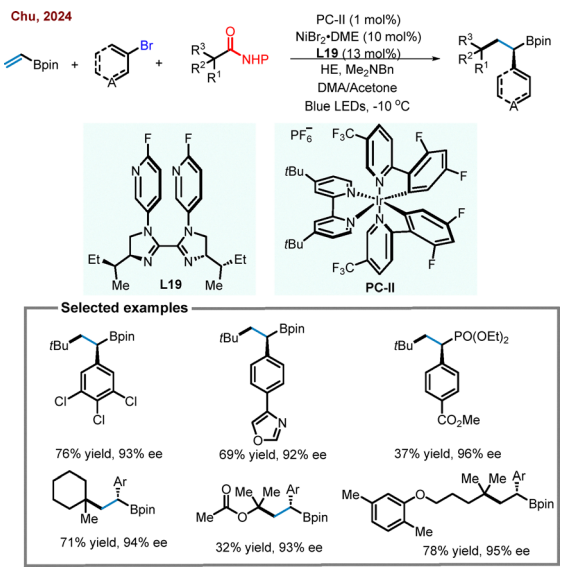

Scheme 16 Nickel/photoredox-catalyzed three-component 1,2-alkylarylation.

expansion to other classes of organoboron reagents, aryl chlorides, and more complex radical precursors will be important for fully generalizing this three-component enantioselective XEC manifold.

2.2 Cobalt/photoredox cooperative catalysis

As an abundant, low-toxicity and cost-effective transition metal, cobalt is also extensively used in diverse transition metal-catalyzed reactions, particularly in asymmetric catalysis.[91] In typical cobalt-catalyzed cross-coupling reactions, the catalytic cycle proceeds *via* oxidative addition of alkyl, alkenyl, or alkynyl halides to an active cobalt species, forming an organocobalt intermediate (Scheme 17a), which is subsequently reduced by stoichiometric reductants such as metals or organic reductants, or *via* hydrogen-atom-transfer (HAT) pathways. The resulting low-valent cobalt species then engage a second alkyl or alkenyl electrophile (*e.g.*, halides or triflates), followed by reductive elimination to furnish the coupled product and regenerate the active catalyst (Scheme 18).[92] Under cooperative photoredox conditions, the reduced photocatalyst can replace traditional reductants to generate low-valent cobalt species or cobalt hydrides *in situ*, thereby streamlining electron delivery and expanding the scope of cobalt-catalyzed reductive transformations (Scheme 17b).

Compared with nickel catalysis, the d-electron configuration of cobalt more readily affords high-spin Co(I)/Co(II) species with pronounced radical characteristics, rendering cobalt inherently suited to radical pathways operating under highly reducing conditions in synergistic visible-light-driven photoredox asymmetric reductive couplings.[93] On one hand, cobalt catalysis excels at activating strongly electrophilic or readily cleavable alkyl precursors *via* single-electron transfer (SET), rapidly generating reactive C(sp^3)-radicals that are trapped by Co(II) species within a chiral ligand environment to afford chiral Co–alkyl intermediates, which undergo stereoselective reductive

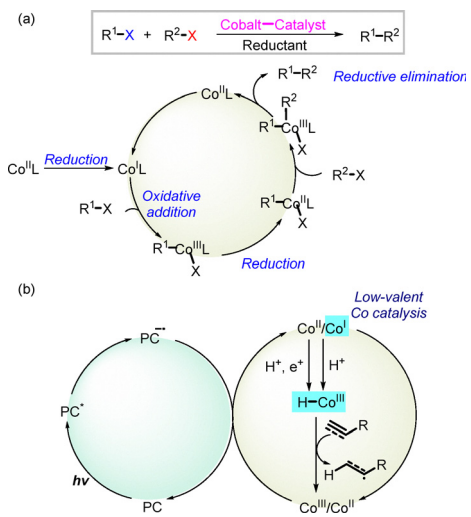

Scheme 17 (a) A general mechanism for Co-catalyzed reductive cross-coupling. (b) Mechanisms for cobalt/photoredox-catalyzed reductive transformations.

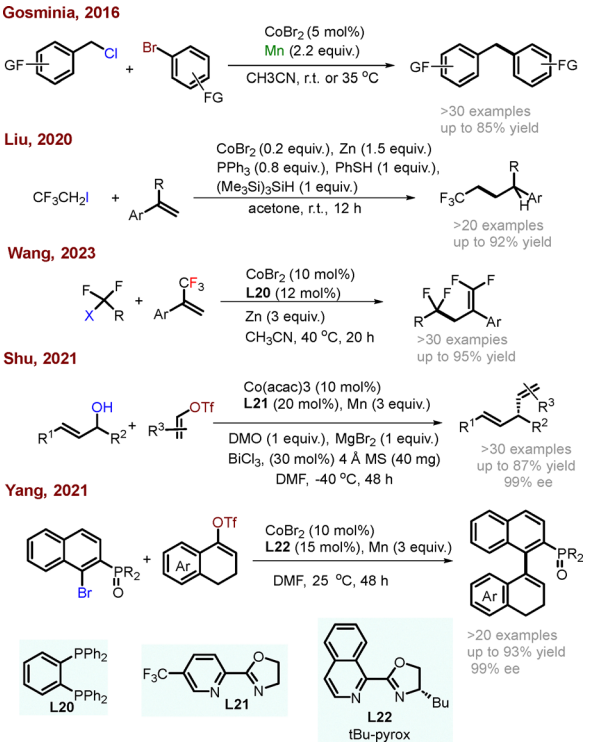

Scheme 18 Co-Catalyzed reductive cross-coupling promoted by stoichiometric reductants.

elimination from high-valent Co(III) to form C(sp^3)–C(sp^3) or C(sp^3)–C(sp^2) bonds. On the other hand, Co(I)/Co(II) species can react with hydrogen donors (*e.g.*, alcohols, amines, organic hydride sources) under photoredox cycling to generate highly reactive Co–H intermediates capable of selective hydrogen-atom transfer or hydrometallation to π systems such as alkenes and alkynes, thereby producing carbon-centered radicals or organocobalt species that subsequently recombine with a second electrophile or photogenerated radical, followed by stereoselective reductive elimination from high-valent cobalt to forge chiral C–C bonds.[94] Overall, cobalt is particularly suited to two representative substrate classes in visible-light-enabled asymmetric reductive coupling: (1) alkyl electrophiles requiring high SET reactivity to release C(sp^3) radicals, and (2) reductive hydrofunctionalization and addition–coupling reactions of alkenes and alkynes, in which a π bond first reacts and then engages in C–C bond formation, thereby offering a reactivity profile that is complementary to nickel systems, which have been most extensively developed for cross-electrophile couplings of (hetero)aryl and alkenyl halides with alkyl partners.

2.2.1 Chiral C_{sp^3}–C_{sp^2} bond formation. Enantioselective reductive couplings between two π-systems have seen substantial development over the past decades.[95] In particular, alkynes, as easily accessible π-components, have been widely employed to construct structurally diverse chiral alkenes.[96] Among them, the reductive coupling of alkynes with aldehydes represents an attractive approach to chiral allylic alcohols, a class of versatile intermediates broadly utilized in organic synthesis and as core motifs in many bioactive natural

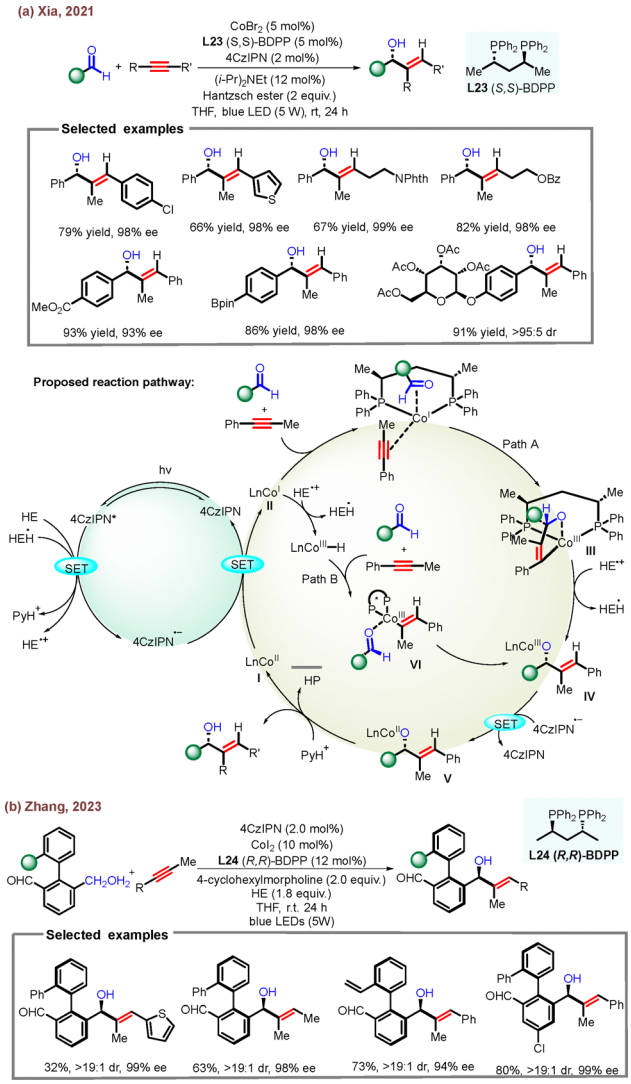

Scheme 19 Co/photoredox-catalyzed reductive coupling of alkynes with aldehydes or alkenyl nitriles.

products and pharmaceuticals. However, their asymmetric variants have been only scarcely reported. In 2021, Xia and co-workers reported a practical cobalt/photoredox-catalyzed reductive coupling of aldehydes and alkynes under mild conditions (Scheme 19a).[97] This method employed asymmetric internal alkynes together with a commercially available photocatalyst 4CzIPN and chiral ligand (*S*,*S*)-BDPP **L23**, enabling the synthesis of diverse allylic alcohols with excellent regio-, stereo-, and enantioselectivities. A variety of (hetero)aryl-substituted internal alkynes and aromatic aldehydes were successfully transformed, and the reaction tolerated several common functional groups. In the tentative mechanism, 4CzIPN* generated by photoexcitation of 4CzIPN can undergo a SET process with Hantzsch ester (HE) to generate 4CzIPN$^{\bullet-}$, which can reduce ligand-mediated [Co^{II}] complex **I** to low-valent [Co^{I}] species **II**. Subsequently, aldehydes and alkynes can be coordinated to [Co^{I}] species **II** followed by oxidative cyclization to afford the oxacobaltacyclopentene intermediate **III**. Then, HE$^{\bullet+}$ proceeds to a protonation reaction generating allylic cobalt alkoxide intermediate **IV** and HEH radical. On the other hand, the HEH radical can also contribute an electron to the photoexcited 4CzIPN*, resulting in the formation of the pyridinium ion PyH^{+} and 4CzIPN$^{\bullet-}$, which can reduce [Co^{III}] intermediate **IV** to [Co^{II}] **V**. Finally, in the presence of PyH^{+}, the target product allyl alcohol is generated. Additionally, there may be another reaction pathway whereby [Co^{I}] **II** can be oxidized by HE^{+} to the [Co^{III}]–H species **VI**, which undergoes a hydrometallation with the alkynes, followed by addition of aldehydes with alkenyl cobalt intermediate to form species **IV**. It is worth noting that analogous Ni/photoredox systems have so far been much less successful for this type of alkyne–aldehyde reductive coupling. In this transformation, the ability of cobalt to access both low-valent Co(I) species and Co–H intermediates under photoredox conditions, and to promote oxidative cyclization between a π bond and a carbonyl group, appears crucial to achieving high efficiency and stereocontrol.

Notably, in 2023, Zhang and co-workers described a similar work in which they provided a modular platform for the synthesis of axially chiral secondary alcohols (Scheme 19b).[98] Despite these advances, current Co/photoredox alkyne-aldehyde couplings are largely restricted to internal aryl-substituted alkynes and aromatic aldehydes, typically require superstoichiometric Hantzsch ester under carefully controlled conditions, and show reduced efficiency with aliphatic partners or strongly coordinating functional groups. Broadening this reactivity to less activated or fully aliphatic π-components and to more densely functionalized substrates therefore represents an important direction for future development.

In addition, asymmetric reductive couplings between alkynes and alkenyl partners remain largely unexplored, even though both classes of substrates are readily available and commonly used in synthesis. A major obstacle in these transformations arises from competing homocoupling pathways of the alkyne or alkene.[99] To date, the only reported example of enantioselective reductive coupling between alkynes and cyclic enones to furnish β-alkenyl cyclic ketones was disclosed by Cheng and co-workers in 2011 (Scheme 20a).[100] Such transformations generally rely on stoichiometric quantities of metallic reductants, such as Zn or Mn powders. Hence, the design of new catalytic systems that can achieve high levels of selectivity in asymmetric alkyne–alkene reductive coupling remains an important objective. In 2022, Xia and co-workers expanded the system to the reductive cross-coupling of internal alkynes and electron-deficient activated alkenes and circumvented the need for stoichiometric metal reductants (Scheme 20b).[101] Compared to previous work, this coupling employed a simple organic base, with water as the hydrogen source, rather than the initially used HE. Various β-chiral homoallylic nitriles were obtained and can be further transformed into chiral building blocks. In 2025, Zhou *et al.* further realized an efficient visible-light-driven cobalt-catalyzed enantioselective RCC reaction between electronically unbiased succinimide-containing cyclobutenes and internal alkynes, overcoming the challenge of β-hydride elimination from cobalt-cyclopentenyl intermediates

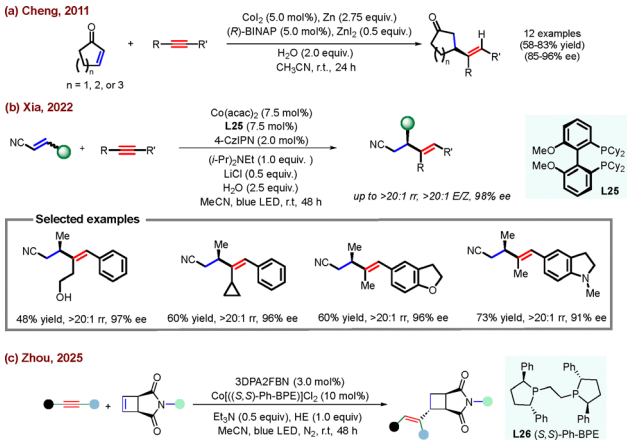

Scheme 20 Co/photoredox-catalyzed reductive coupling of alkynes with alkenes.

leading to 1,4-dienes (Scheme 20c).[102] This strategy afforded enantioenriched vinylcyclobutanes with excellent enantioselectivity, as well as good stereoselectivity and regioselectivity. Nevertheless, current Co/photoredox alkyne-alkene coupling systems are largely confined to internal aryl-substituted alkynes in combination with activated Michael acceptors or specially designed succinimide-containing cyclobutenes, and typically require carefully tuned ligand–base combinations. Their performance with simple terminal alkenes or alkynes, highly functionalized substrates, or strongly coordinating functional groups remains underexplored, indicating that considerable scope for broadening substrate generality and reaction robustness still exists.

Chiral benzyl alcohols represent an important structural motif that is broadly found in natural products, pharmaceuticals, and functional materials.[103] Therefore, developing efficient and practical synthetic approaches to these compounds has long been a central pursuit in organic chemistry. However, the direct enantioselective coupling of aryl halides with aldehydes to access optically pure alcohols has remained a formidable challenge. A breakthrough was made in 2019, when Ohmiya and co-workers realized this transformation through a dual Pd/Cu catalytic system (Scheme 21a).[104] In this approach, aromatic aldehydes were first converted into enantioenriched α-alkoxyalkyl anions *via* asymmetric Cu catalysis, which subsequently underwent Pd-catalyzed stereospecific cross-coupling with aryl halides. In 2022, Xiao and co-workers demonstrated a visible light-mediated cobalt-catalyzed asymmetric reductive Grignard-type addition between aldehydes and aryl iodides to yield a series of chiral benzyl alcohols under mild reaction conditions without relying on stoichiometric metallic reductants or precious-metal catalysts (Scheme 21b).[105] The method could be utilized for the synthesis of chiral 1,2-amino alcohols and the chiral drug D-cloperastine. As shown in the proposed mechanism, under visible light irradiation, photoexcited 4CzIPN* undergoes one-electron reduction in the presence of HE, generating the reduced 4CzIPN$^{\bullet-}$, which can convert [Co^{II}] complex **I** into [Co^{I}]

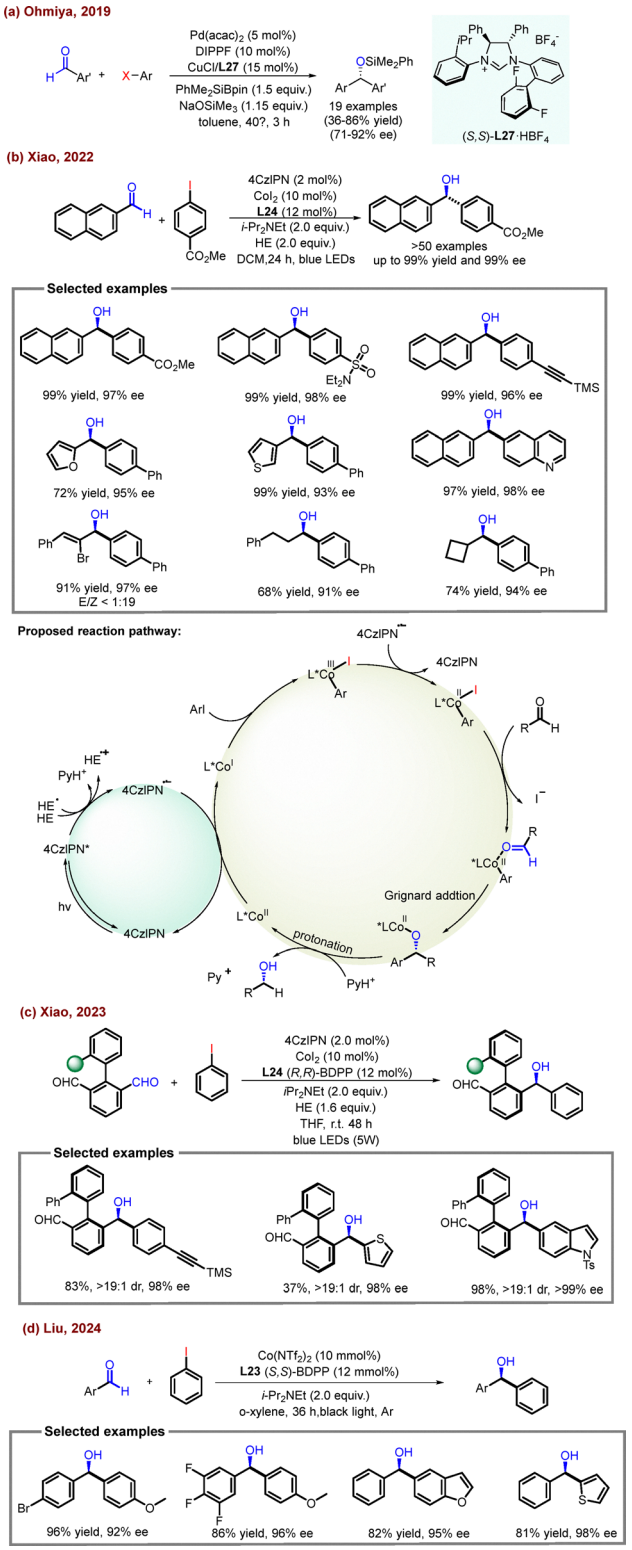

Scheme 21 Visible light-mediated cobalt-catalyzed asymmetric reduction of aldehydes with aryl iodides.

species **II** by a SET process. Next, oxidative addition of the aryl iodide to [Co^{I}] species **II** produces the aryl [Co^{III}] intermediate **III** and subsequent reduction of aryl [Co^{III}] intermediate with another 4CzIPN$^{\bullet-}$ yields aryl [Co^{II}] complex **IV**. Following

coordination with the aldehyde, the aryl [Co^{II}] complex **V** undergoes a Grignard-type addition with the carbonyl to give a chiral alcohol anion. Finally, protonation occurs to obtain the target product as well as [Co^{II}] complex **I**, completing the catalytic cycle. However, this system requires superstoichiometric Hantzsch ester, which impacts both cost and atom economy. In 2023, this group further expanded the applicability of this asymmetric metallaphotoredox catalysis by realizing the construction of axial and central chirality simultaneously (Scheme 21c).[106] They described a visible light-driven cobalt-catalyzed asymmetric reductive cross-coupling of biaryl dialdehydes with aryl iodides to yield a broad range of alcohols in generally high yields and with excellent enantioselectivity by the combination of axially chiral biphenyl and centrally chiral alcohol. In 2024, Liu and co-workers further developed the system to light-promoted Co-catalyzed asymmetric RCC of aryl iodides and aromatic aldehydes with widespread commercial chemical *i*-Pr_2NEt as the reductant to yield a variety of chiral diaryl carbinols with excellent yields and enantioselectivities (Scheme 21d).[107] Moreover, this approach circumvented the need for excess Hantzsch ester previously required, thereby addressing issues related to cost and atom economy. Despite these advances, current Co/photoredox protocols for aryl halide-aldehyde couplings are mainly limited to aromatic aldehydes and aryl iodides, rely on superstoichiometric organic reductants (HE or i-Pr_2NEt), and show reduced efficiency or selectivity in the presence of strongly coordinating or highly electron-deficient functional groups. Extension to aliphatic aldehydes, more complex polyfunctional substrates, and alternative aryl electrophiles (*e.g.* aryl chlorides) remains an important goal for further broadening the synthetic utility of these methods.

In 2022, Xiao, Lu and co-workers developed a visible-light-induced RCC of racemic heterobiaryls and readily available organic halides, using 4CzIPN as a photocatalyst, **L28** as a rigid, multidentate chiral ligand, $CoCl_2$ as a metal catalyst, and HE as a reducing reagent (Scheme 22a).[108] The utilization of chiral polydentate ligand is key to achieving high yields and excellent enantioselectivity for a variety of axially chiral heteroaromatics. However, asymmetric reductive conjugate addition reactions catalyzed by transition metals remain underdeveloped, mainly due to the lack of broadly applicable catalytic strategies.[109] Only limited examples have been disclosed, primarily involving Pd-[110] or Ni-[111] catalyzed intramolecular processes that rely on specifically designed substrates. A notable advance was recently reported by Zhou and co-workers, who realized the first intermolecular enantioselective reductive conjugate addition of aryl halides to enones under nickel catalysis.[112] The success of this approach relied on a cyclic 1,4-addition pathway, wherein a chiral aryl–Ni(I) species engaged the enone to forge the stereogenic center. To date, these methodologies have mainly focused on generating stereocenters *via* conjugate addition to alkenes, while the construction of axial chirality directly from aryl halides remains unexplored. In 2023, Xiao and co-workers reported a photo-promoted cobalt-catalyzed reductive conjugate addition of heterobiaryls and conjugated alkenes

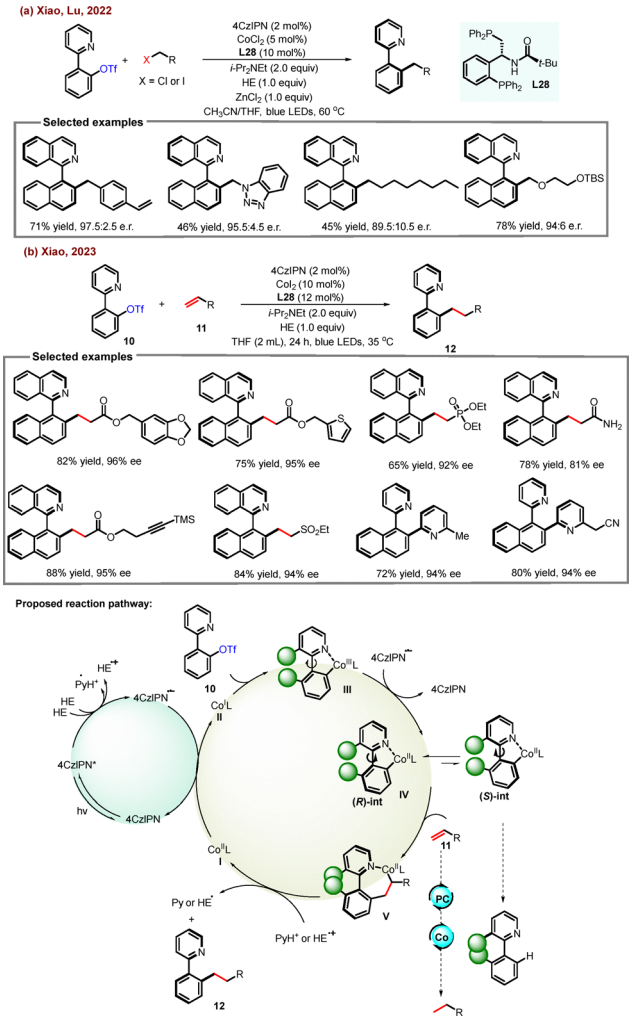

Scheme 22 Photoinduced Co-catalyzed dynamic kinetic asymmetric transformation of racemic heterobiaryls.

under mild and green conditions to afford various axially chiral heterobiaryls (Scheme 22b).[113] This method features excellent functional group tolerance and enantiomeric control. In the depicted postulated catalytic cycle, under blue light irradiation, 4CzIPN in the excited state accepts one electron from HE, generating 4CzIPN$^{\bullet-}$, which reduces the [Co^{II}]/**L28** complex **I** to the [Co^{I}]/**L28** species **II** and regenerates the 4CzIPN by single electron transfer. Subsequently, the oxidative addition of the racemic heterobiaryl triflates **10** with [Co^{I}]/**L28 II** produces the [Co^{III}]/**L28** intermediate **III**, which was then reduced by 4CzIPN$^{\bullet-}$ to produce the [Co^{II}]/**L28** complex **IV**. Coordination of [Co^{II}] with an N atom in the ligand decreases the rotational energy barrier of the axially chiral Co intermediate, resulting in the conversion of (*S*)-int to predominantly (*R*)-int. Next, alkene **11** with [Co^{II}]/**L28** intermediate **IV** undergoes a migratory insertion followed by a protonation process to give the target product **12** and regenerate [Co^{II}]/**L280** intermediate **I** to complete the catalytic cycle. Nevertheless, current Co/photoredox reductive conjugate addition systems for constructing axial chirality remain limited in several respects: (1) they rely

predominantly on heterobiaryl triflates bearing well-defined rotational axes, and electronically or sterically unbiased biaryls remain challenging; (2) aliphatic alkenes and unactivated alkenes typically exhibit low reactivity or poor selectivity; (3) superstoichiometric HE is still required, affecting atom economy; and (4) strongly coordinating or densely functionalized substrates tend to interfere with cobalt speciation or disrupt the delicate rotation–inversion dynamics needed for stereocontrol. Future advances will benefit from catalyst designs that enable broader substrate generality, reduced reliance on stoichiometric reductants, and more predictable stereochemical outcomes across diverse ligand frameworks.

2.2.2 Chiral C_{sp^3}–C_{sp^3} bond formation. Asymmetric reductive coupling of two π-unsaturated pronucleophiles has proved to be a valuable tool for building complex skeletons with great atom economy.[114] In 2023, Maji *et al.* disclosed an example of dual cobalt- and visible-light-induced asymmetric ene–ene reductive coupling reaction between heterobicyclic alkenes and vinyl electrophiles (Scheme 23).[115] The reaction can afford a range of desymmetrized products in high yields, stereoselectivities and enantioselectivities. Generally, C-B bonds can be stereospecifically transformed into various carbon–carbon or carbon–heteroatom bonds (*e.g.*, C–N, C–O bonds, *etc.*), which play an essential role in the construction of complex molecules.[116] Nevertheless, this Co/photoredox ene-ene coupling has so far been demonstrated mainly for heterobicyclic alkenes and activated vinyl electrophiles, and its applicability to simpler or more densely functionalized π-substrates remains to be established.

In 2024, Gong and co-workers demonstrated a cobalt/photoredox-catalyzed diastereo- and enantioselective reductive cross-coupling of diverse aryl or α,β-unsaturated aldehydes and C═O or C═N partners, such as aldehydes, α-keto esters, aryl ketones and *N*-acylhydrazines, enabling the construction of unsymmetrical 1,2-diol derivatives and chiral β-amino alcohols in high yields (Scheme 24).[117] In this system, the authors utilized the differences in nucleophilicity and electrophilicity between iminyl compounds and/or α,β-unsaturated aldehydes, enabling the reaction to proceed in an orderly manner. Due to the poor electrophilicity of iminyl compounds, after coordinating with the reductive cobalt(II) complex, its electron-accepting ability was significantly enhanced, allowing the cobalt-iminyl complex to preferentially undergo single-electron transfer with the Ir(II) complex, and subsequently be able to further react with the electrophilic aldehydes. Despite the broad range of aldehydes and carbonyl/imine partners demonstrated, this protocol is currently limited mainly to aryl and α,β-unsaturated aldehydes and activated C═O/C═N electrophiles, and relies on dual Co/Ir catalysis with stoichiometric Hantzsch ester as the reductant. Its generality toward aliphatic aldehydes, more strongly coordinating or densely functionalized substrates, and alternative reductants remains to be established.

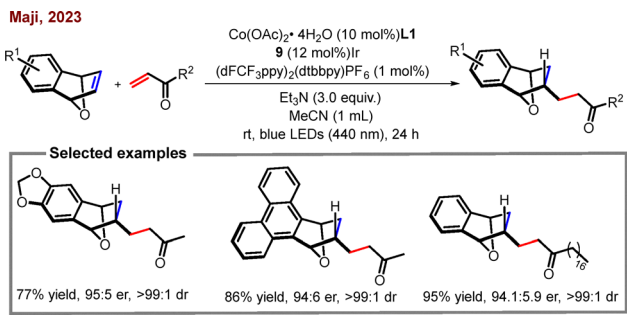

Scheme 23 Cobalt- and visible-light-induced asymmetric ene–ene reductive coupling.

2.3 Palladium/photoredox cooperative catalysis

Palladium occupies a distinct position among transition metals used in cooperative photoredox catalysis.[118] In contrast to nickel and cobalt, which readily engage in one-electron processes and radical-chain-type cross-electrophile couplings, palladium catalysis is traditionally dominated by two-electron oxidative addition/reductive elimination manifolds and π-allyl or π-benzyl chemistry.[119] Under visible-light-driven conditions, Pd^0/Pd^{II} cycles can be merged with photoredox catalysis to access odd-electron Pd species (*e.g.*, Pd^I and Pd^{III}) intermediates that enable radical pathways, while still preserving the well-established platforms for stereocontrol provided by chiral ligands. As a consequence, dual Pd/photoredox catalysis is particularly effective for allylic and benzylic substitution reactions, where π-allyl or π-benzyl Pd intermediates can be combined with photochemically generated radicals to build C(sp^3)–C(sp^3) bonds in an enantioselective fashion.[120,121]

In 2021, Yu and co-workers reported a palladium/photoredox catalyzed reductive homocoupling of allylic acetates using HE or *N*,*N*-diisopropylethylamine (DIPEA) as the reductant, affording various C_2-symmetrical chiral 1,5-dienes in high yields, good regio- and enantioselectivities (Scheme 25a).[120] In the proposed mechanism, visible light excitation of the [Ir^{III}] complex gives an excited state ([Ir^{III}]*), which generates the [Ir^{II}] complex by reductive quenching of DIPEA. On the one hand, the oxidative addition of Pd^0L* **I** with allyl acetate **16** yields (π-allyl)Pd^{II}L* complex **II**. Next, complex **II** can be reduced by the [Ir^{II}] complex to the (π-allyl)Pd^IL* complex **III**, which is in dynamic equilibrium with the Pd^0 species and the allylic radical species **VII**. Complex **III** can continue to undergo oxidative addition with another molecule of allylic acetate **16** to give bis(π-allyl)Pd^{III} complex **IV**, which can be in dynamic equilibrium with bis(η^1-allyl)Pd^{III} complex **V**. In addition, the allylic radical species **VII** can be captured by complex **II** to generate **IV/V**. The **IV/V** complex subsequently undergoes reductive elimination to produce the target homocoupling product **17** and the Pd^IL* species **VI**, which can be reduced to regenerate Pd^0L* **I**, completing the catalytic cycle. Shortly thereafter, this group further extends the system to the dual photo-induced palladium catalyzed highly regio- and enantioselective reductive coupling of tertiary/secondary alkyl bromides with allylic acetates using HE as the homogeneous organic reductant, realizing the construction of chiral C_{sp^3}–C_{sp^3} bonds (Scheme 25b).[121] The method enabled the construction of quaternary carbon centers in moderate to excellent yields,

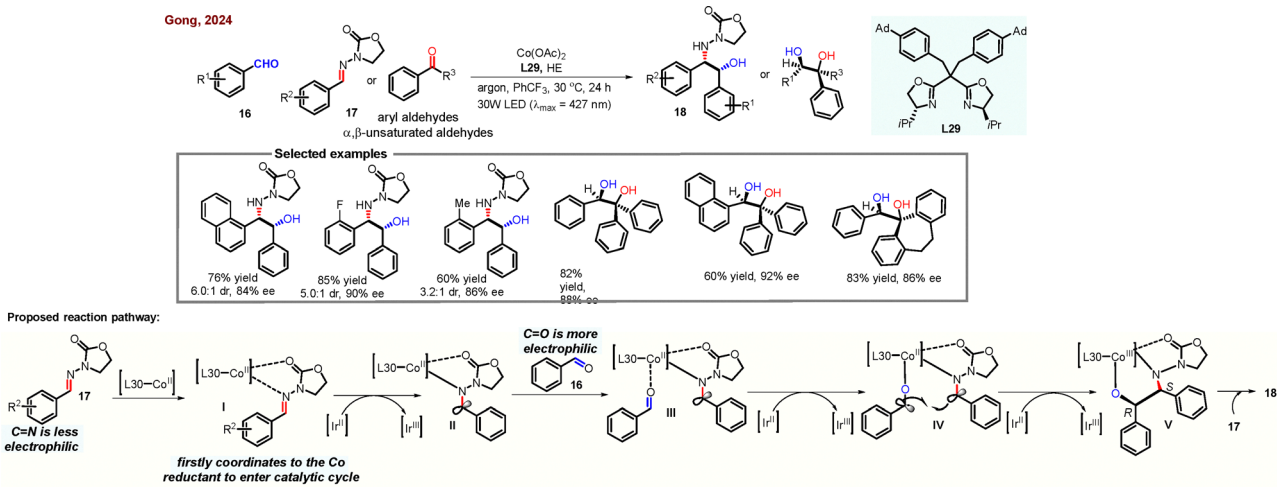

Scheme 24 Enantioselective reductive cross-coupling of aryl aldehydes or α,β-unsaturated aldehydes.

broadening the scope of traditional transition metal-catalyzed reductive allylic alkylation.

Nevertheless, these Pd/photoredox protocols are currently restricted mainly to allylic acetates as π–allyl precursors and to specific tertiary or secondary alkyl bromides, and they rely on precious-metal photocatalysts and stoichiometric organic reductants. Their generality toward more diverse allylic leaving groups, other alkyl electrophiles, and more densely functionalized or strongly coordinating substrates remains to be fully established.

2.4 Titanium/photoredox cooperative catalysis

Titanium exhibits a mechanistically distinct profile compared with the other transition metals discussed in this review. As an early transition metal with pronounced oxophilicity, Ti(IV) complexes can be photochemically reduced to Ti(III) species, which are highly potent single-electron reductants capable of generating metal-bound ketyl radicals from carbonyl compounds.[122] In classical stoichiometric titanium chemistry, this mode of reactivity underpins McMurry couplings and pinacol-type reactions.[123] Under cooperative photoredox conditions, titanium is thus particularly well suited for carbonyl-centered reductive transformations, in which Ti(III)-ketyl radical intermediates undergo stereoselective C–C bond formation to furnish 1,2-diols and related products, thereby complementing late-transition-metal systems that predominantly engage in cross-electrophile couplings of halides or π-unsaturated partners.

In 2022, Cozzi's group reported a photo-induced pinacol coupling of aromatic aldehydes promoted by non-toxic, available and cheap titanium complexes, providing the chiral 1,2-diols in a single step (Scheme 26).[124] This transformation is enabled by a red-absorbing dimethoxyquinacridinium dye **18** under orange light irradiation, which facilitates the photoreduction of Ti(IV) to Ti(III), followed by the generation of titanium-bound ketyl radicals that undergo stereoselective coupling. A chiral Ti(Salen) complex allows for effective enantioinduction, affording products with good enantiomeric excesses. In this method, functional groups such as halogen, naphthyl, methoxyl, and others are tolerated. Nevertheless, the current protocol has mainly been demonstrated for aromatic aldehydes under a specific Ti(Salen)/organic-dye system, and its extension to aliphatic carbonyl compounds, more densely functionalized substrates, or alternative titanium manifolds remains to be explored.

2.5 Rhodium/photoredox cooperative catalysis

Although studies employing chiral transition-metal complexes remain relatively limited, they nonetheless provide a compelling and potentially powerful chiral manifold for asymmetric catalysis.[125] These systems rely on "metal-centered chirality," wherein asymmetric coordination of ligands around an octahedral metal center generates intrinsic chirality and imparts a well-defined three-dimensional configuration to the complex.[126] Despite these conceptual advantages and the appealing flexibility in molecular design, reported examples of asymmetric reductive transformations mediated by transition-metal complexes remain exceedingly rare, with both substrate classes and reaction patterns still narrowly defined, indicating that this field is at an early stage of development and offers considerable room for conceptual expansion and methodological advancement.

In 2017, Meggers and co-workers utilized a chiral bis-cyclometalated Rh(III) complex to achieve stereocontrol over photo-generated carbon-centered radical reactions, enabling the enantioselective radical allylation between α,β-unsaturated *N*-acylphthalimides and allyl sulfones (Scheme 27a).[127] Mechanistically, the Rh-coordinated Michael acceptor I, under the conditions of inexpensive and readily available Hantzsch ester as a photoredox mediator, undergoes selective photoinduced single-electron reduction to generate a Rh-coordinated prochiral radical II, which is then highly stereoselectively trapped by allyl sulfones to generate intermediate III. The resulting β-scission releases sulfonyl radicals, generating intermediate IV, which subsequently

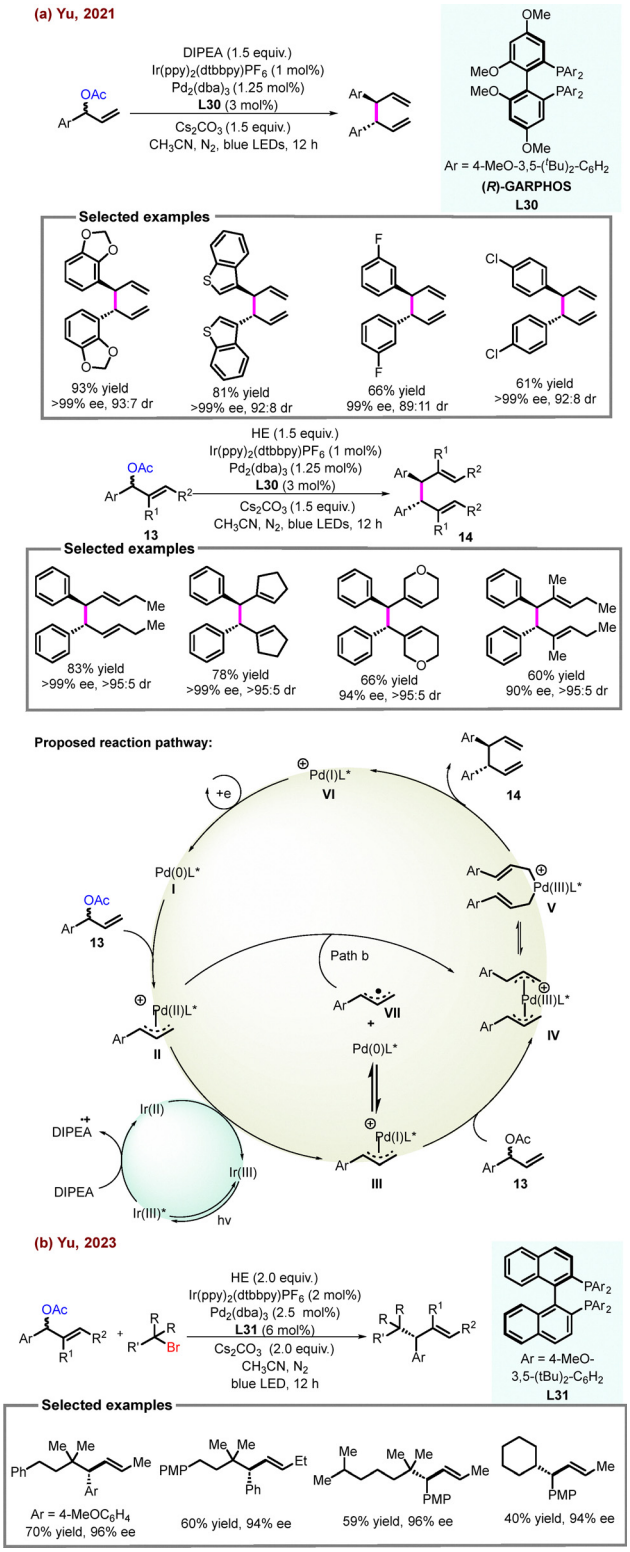

Scheme 25 Palladium/photoredox catalyzed reductive coupling of allylic acetates.

undergoes protonation to yield the allylation product. Subsequently, they further disclosed a formally "photocatalyst-free" single-metal system in which a chiral-at-metal Rh(III) complex governs both substrate activation and stereocontrol in the

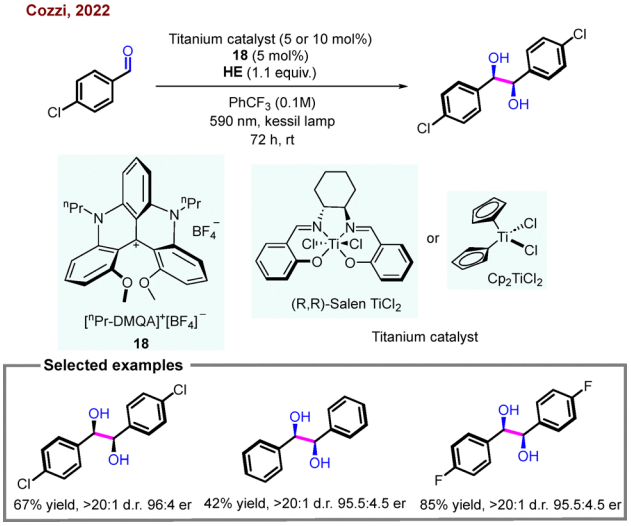

Scheme 26 Photo-induced pinacol coupling of aromatic aldehydes.

visible-light-driven reductive conjugate addition of glycine-derived *N*-(acyloxy)phthalimides to α,β-unsaturated *N*-acylpyrazoles, delivering a broad range of β-substituted γ-aminobutyric acid derivatives in high yields and ee values (Scheme 27b).[128] In this manifold, Hantzsch ester serves as the photoexcited reductant under compact fluorescent light irradiation, while the Rh complex functions as a Lewis acid template and chiral environment, thus embodying the concept of single-metal asymmetric photocatalysis in a synthetically valuable setting. However, the methodology remains largely confined to *N*-acylpyrazole Michael acceptors and *N*-(acyloxy)phthalimide radical precursors, requires over-stoichiometric Hantzsch ester, and is sensitive to oxygen, so its generality is still limited and the precise nature of the photoactive species and elementary steps has not been fully elucidated. Consequently, this contribution should be viewed as an illustrative yet still early example, underscoring that asymmetric reductive photochemistry with single chiral transition-metal photocatalysts is only beginning to emerge and leaves ample space for further methodological and mechanistic development.

3 Cooperative photoredox and enzyme dual catalysis

Enzymes are appealing catalysts for enantioselective synthesis because of their ability to mediate reactions with an unprecedented level of stereochemical control.[129] However, due to the fact that natural enzymes cannot directly catalyse reductive cross-coupling reactions, there is an urgent need to develop an alternative reductive coupling mechanism that is compatible with current enzyme systems. In 2020, Hyster and coworkers developed an asymmetric reductive cyclization of alkyl iodides to yield chiral esters and amides (Scheme 28).[130] Flavin-dependent "ene"-reductases (EREDs) can catalyze this process with high enantioselectivity through the formation of a charge transfer (CT) complex between the flavin and the alkyl iodide substrates. Photoexcitation of this complex generates

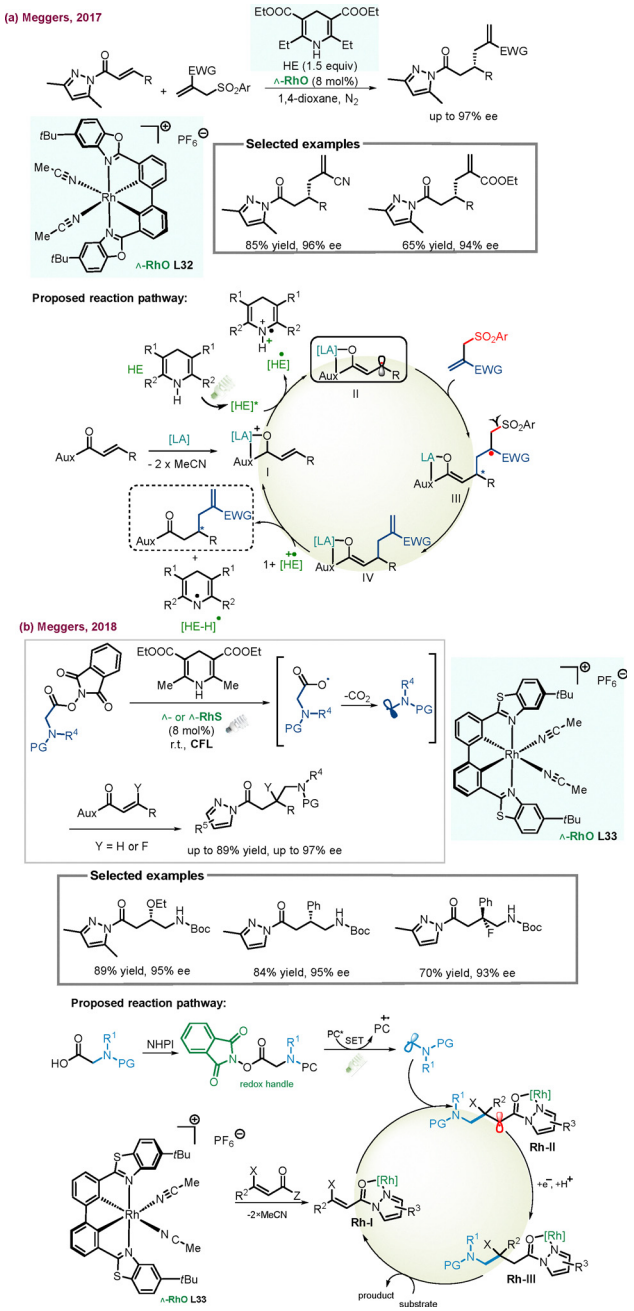

Scheme 27 Rhodium/photoredox catalyzed reductive coupling.

unstabilized nucleophilic alkyl radical, followed by an intramolecular cyclization, and subsequently the stereoselective transfer of hydrogen atom (HAT) from the flavin semiquinone (FMN_{sq}) to build the α-stereocenter.

In 2022, Hyster *et al.* also demonstrated unprecedented photoenzymatic highly enantioselective and chemoselective $C(sp^3)$–$C(sp^3)$ XECs between nitroalkanes and alkyl halides (Scheme 29).[131] In this reaction, the target products can be obtained in moderate to excellent yields under cyan light irradiation using flavin-ERED catalysis, where cyan light, ERED and the NADPH (reduced form of nicotinamide adenine dinucleotide phosphate) regeneration system (GDH/NADP+/glucose)

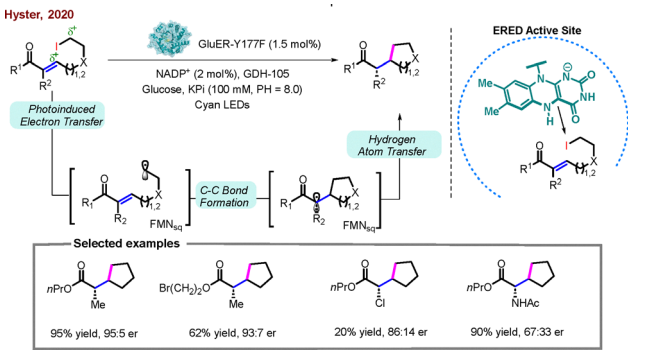

Scheme 28 Visible-light-promoted enzymes catalyzed asymmetric reductive cyclization of alkyl iodides.

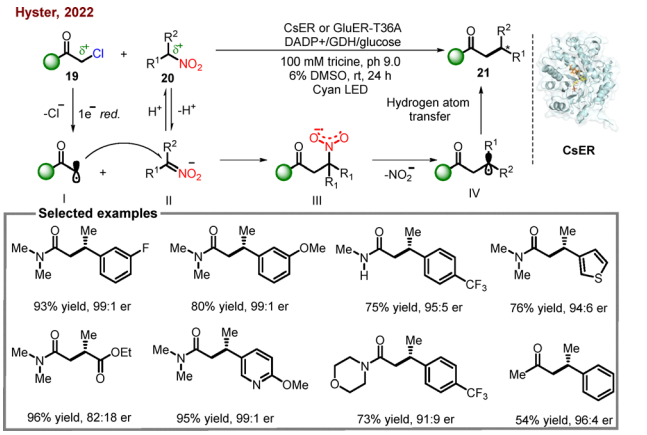

Scheme 29 Visible-light-promoted enzymes catalyzed $C(sp^3)$–$C(sp^3)$ XECs between nitroalkanes and alkyl halides.

are crucial for the reactivity. Regarding the mechanism, the reduction of alkyl halide **19** yields alkyl radical **I**, which reacts with nitrate **II** generated *in situ* to generate a new C–C bond and nitro radical anion **III**. Enzyme-mediated homolytic cleavage of the C–N bond leads to the formation of nitrite and alkyl radical **IV**, which can undergo a HAT process to give cross-coupling product **21**. Moreover, this reaction exhibits good functional group compatibility, including fluorine, trifluoromethyl, methoxy, thiophene, pyridine, ester groups and so on.

However, current photoenzymatic reductive cross-couplings remain limited to flavin-dependent ERED systems, require continuous light and cofactor-recycling machinery, and have been demonstrated mainly for activated alkyl halides and nitro-containing partners. Expanding these methods to broader electrophile classes, aliphatic substrates, and more synthetically diverse bond constructions remains an important challenge.

4 Cooperative photoredox and hydrogen-bonding catalysts

Chiral phosphoric acids (CPAs) are some of the most valuable organocatalysts contributing significantly to the development

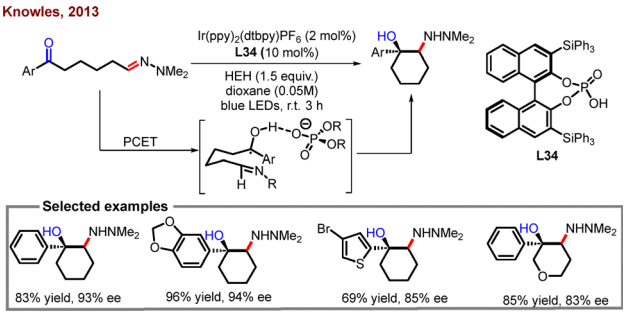

Scheme 30 Cooperative photoredox and hydrogen bonding catalysts for the enantioselective reductive couplings of hydrazones and ketones.

of high-efficiency platforms for asymmetric reactions during the past two decades.[132] Most CPA-promoted asymmetric reactions involve non-covalent interactions, such as the formation of hydrogen bonds, which proceed to the next step in a stereotactic manner. With their adaptable interaction patterns, tunable properties and remarkable stability against hydrolysis and oxidation, CPAs are ideal candidates for synergistic interactions with photocatalysts. The effectiveness of these methods has been extensively proved in numerous studies. In 2013, Knowles and co-workers demonstrated a highly enantioselective intramolecular reductive cross-coupling of hydrazones and ketones, enabling the successful synthesis of a series of 1,2-aminoalcohol derivatives (Scheme 30).[133] This reaction, utilizing $Ir(ppy)_2(dtbpy)PF_6$ as the photoredox catalyst, aryl phosphoric acid as the ligand, and HEH as the reducing agent, mainly involved neutral ketyl radical generated *via* a PCET process. Notably, these neutral keto radicals seemed to remain H-bonded to the chiral conjugate group of the Brønsted acid, contributing to the generation of target products with excellent yields and enantioselectivities. However, current CPA/photoredox reductive coupling examples are largely restricted to intramolecular processes and specific hydrazone–carbonyl manifolds under Ir/HEH conditions, and their generality toward intermolecular couplings and broader substrate classes remains to be established.

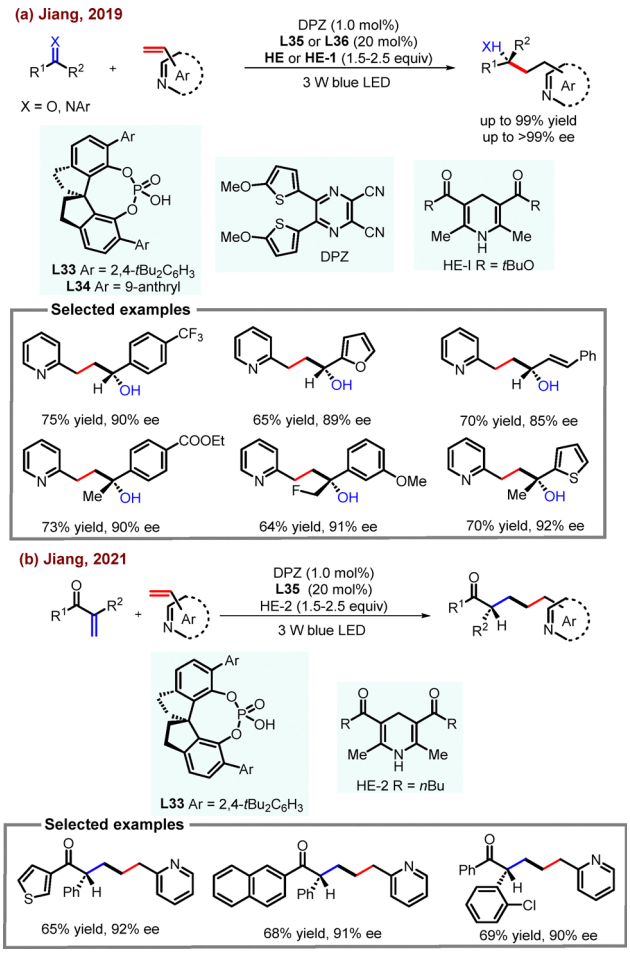

Scheme 31 Cooperative photoredox and hydrogen bonding catalysts for the enantioselective reductive couplings of vinylpyridines with aldehydes, ketones, and imines.

Structurally varied azaarene derivatives are widely found in pharmaceuticals, natural products, and functional materials, as well as being essential ligands and catalysts.[134] In 2019, Jiang and co-workers focused on the synthesis of various chiral γ-secondary/tertiary hydroxyl and amino-substituted pyridines through a visible-light-mediated highly enantioselective reductive coupling of vinylpyridines with ketones, aldehydes and imines (Scheme 31a).[135] It was notable that the CPA was employed to activate the substrate and control the stereoselectivity through the hydrogen bonding interactions. Shortly after, they further extended the system to the enantioselective reductive cross coupling of 2-vinylazaarenes and α-branched vinylketones (Scheme 31b).[136] By constructing a bicatalytic system using dicyanopyrazine-derived chromophore (DPZ) as a photosensitiser, HE as the reducing agent and in the presence of SPINOL-based CPA, they obtained enantioenriched aziridines and their derivatives exhibiting stereocenters at the remote δ-position in high yields and excellent enantiomeric excesses. α-Phenyl vinyl ketones bearing different substituents and 2-vinylpyridines with various electron-rich and electron-deficient substituents are well tolerated under the standard conditions.

Despite their conceptual elegance, many of these CPA-based dual catalytic systems require relatively high catalyst loadings and are restricted to substrates bearing strongly polarized carbonyl or azaarene motifs. Extending hydrogen-bond-directed enantioselective reductions to less activated electrophiles remains a significant challenge.

5 Conclusion and outlook

Synergistic catalysis, which activates two reacting partners simultaneously through separate catalysts to achieve new or elusive chemical transformations, is a valuable synthetic strategy. In this tutorial review, we highlighted the recent advances in enantioselective reductive couplings under cooperative photoredox catalysis. These advances were briefly summarized based on the classification of catalytic models: (a) cooperative

photoredox and transition-metal dual catalysis, (b) cooperative photoredox and enzyme dual catalysis, and (c) cooperative photoredox and hydrogen-bonding catalysis. These successful strategies offer new protocols for the efficient and enantioselective synthesis of valuable chiral organic compounds. The developments highlighted in this review will play a guiding role for researchers aiming to enter this area. Despite the progress made in enantioselective reductive transformations under photoredox catalysis, many challenges and opportunities still remain, offering ample room for further investigation: (1) in the reported synergistic catalytic modes, nickel remains the preferred choice, and other transition metal catalysts and their reactivity are yet to be further developed. (2) Nickel-catalyzed RCC has emerged as a powerful strategy for C–C bond construction, yet several fundamental challenges remain. The origin of chemoselectivity when engaging two structurally similar electrophiles, particularly in $C(sp^3)$–$C(sp^3)$ and $C(sp^2)$–$C(sp^2)$ couplings, has yet to be fully elucidated, and in many cases one coupling partner must be used in significant excess to obtain practical yields. In addition, the transition from stoichiometric metallic reductants such as Zn or Mn to sustainable and nonmetallic alternatives is still in its infancy, despite the potential benefits for large-scale synthesis and the reduction of residual metal impurities in pharmaceutical production. (3) Electrophilic reagents are still limited to aryl/alkyl halides, and their scope needs to be further expanded. (4) Compared to visible light/transition-metal co-catalysis, visible light/enzyme catalysis and visible light/hydrogen bonding catalysts have yet to be fully explored. (5) Lastly, there is still a high demand in synthetic community for applying these strategies to achieve the synthesis of highly valued molecules. We believe that the development of new and efficient catalytic systems is crucial for addressing these challenges.

As photochemistry becomes an increasingly popular and powerful synthetic tool, the development of new dual-catalytic methods will certainly continue to be a promising strategy for the visible-light induced construction of complex chiral organic molecules. We also highly believe that more rationally designed new reductive transformations under photoredox co-catalysis are expected to be discovered in the near future.

Author contributions

Y. S. and D. Y. wrote the paper.

Conflicts of interest

There are no conflicts to declare.

Data availability

No primary research results, software or code have been included and no new data were generated or analysed as part of this review.

Acknowledgements

We acknowledge financial support from the National Natural Science Foundation of China (22271170), the Taishan Scholars Program from Shandong Province (tsqn202408197), the Natural Science Foundation of Shandong Province (ZR2024QB154) and the Scientific Research Foundation of Qingdao University of Science and Technology.

Notes and references

1 B. M. Trost, *Proc. Natl. Acad. Sci. U. S. A.*, 2004, **101**, 5348–5355.
2 H. C. Kolb, M. S. VanNieuwenhze and K. B. Sharpless, *Chem. Rev.*, 2002, **94**, 2483–2547.
3 W. S. Knowles, *Angew. Chem., Int. Ed.*, 2002, **41**, 1998–2007.
4 D. Chusov, G. A. Molander, V. Ratovelomanana-Vidal, O. Riant and E. Schulz, *ACS Catal.*, 2023, **13**, 11494–11508.
5 R. Noyori, *Angew. Chem., Int. Ed.*, 2002, **41**, 2008–2022.
6 (*a*) T. P. Yoon and E. N. Jacobsen, *Science*, 2003, **299**, 1691–1693; (*b*) A. Pfaltz and W. J. Drury III, *Proc. Natl. Acad. Sci. U. S. A.*, 2004, **101**, 5723–5726.
7 (*a*) C. Aubert, L. Fensterbank, P. Garcia, M. Malacria and A. Simonneau, *Chem. Rev.*, 2011, **111**, 1954–1993; (*b*) W. Deng, Y. Liu, J. Shen, Q. Wang, Y. Chen and J. Zhang, *Chin. J. Org. Chem.*, 2022, **42**, 3051; (*c*) Z. Miao, Y. Gao and Y. Mao, *Chin. J. Org. Chem.*, 2022, **42**, 1904.
8 A. H. Cherney, N. T. Kadunce and S. E. Reisman, *Chem. Rev.*, 2015, **115**, 9587–9652.
9 (*a*) J. Wen, F. Wang and X. Zhang, *Chem. Soc. Rev.*, 2021, **50**, 3211–3237; (*b*) Y. Y. Li, S. L. Yu, W. Y. Shen and J. X. Gao, *Acc. Chem. Res.*, 2015, **48**, 2587–2598.
10 B. Yao, J. Wu, Y. Wang and H. Jiang, *Chin. J. Org. Chem.*, 2020, **40**, 3044.
11 (*a*) C. G. Newton, S. G. Wang, C. C. Oliveira and N. Cramer, *Chem. Rev.*, 2017, **117**, 8908–8976; (*b*) C. X. Liu, W. W. Zhang, S. Y. Yin, Q. Gu and S. L. You, *J. Am. Chem. Soc.*, 2021, **143**, 14025–14040; (*c*) Q. Zhang, L.-S. Wu and B.-F. Shi, *Chem*, 2022, **8**, 384–413.
12 (*a*) M. S. Taylor and E. N. Jacobsen, *Angew. Chem., Int. Ed.*, 2006, **45**, 1520–1543; (*b*) M. Renio and M. R. Ventura, *Org. Biomol. Chem.*, 2025, **23**, 7521–7537; (*c*) S. Vera, A. García-Urricelqui, A. Mielgo and M. Oiarbide, *Eur. J. Org. Chem.*, 2023, e202201254; (*d*) A. G. Doyle and E. N. Jacobsen, *Chem. Rev.*, 2007, **107**, 5713–5743.
13 (*a*) M. Alfaro Blasco and H. Groger, *Bioorg. Med. Chem.*, 2014, **22**, 5539–5546; (*b*) N. G. Schmidt, E. Eger and W. Kroutil, *ACS Catal.*, 2016, **6**, 4286–4311; (*c*) P. Clapés and X. Garrabou, *Adv. Synth. Catal.*, 2011, **353**, 2263–2283.
14 K. Hult and P. Berglund, *Trends Biotechnol.*, 2007, **25**, 231–238.
15 H. Zhao, *RSC Adv.*, 2024, **14**, 25932–25974.
16 (*a*) X. Y. Yu, J. R. Chen and W. J. Xiao, *Chem. Rev.*, 2021, **121**, 506–561; (*b*) A. Gómez-Suárez, S. P. Pitre and C. Zhu, *ChemCatChem*, 2024, **16**, e202401079.

17 (*a*) J. M. Narayanam and C. R. Stephenson, *Chem. Soc. Rev.*, 2011, **40**, 102–113; (*b*) M. H. Shaw, J. Twilton and D. W. C. MacMillan, *J. Org. Chem.*, 2016, **81**, 6898–6926; (*c*) G. Ciamician, *Science*, 1912, **36**, 385–394.
18 L.-L. Liao, L. Song, S.-S. Yan, J.-H. Ye and D.-G. Yu, *Trends Chem.*, 2022, **4**, 512–527.
19 (*a*) W. Kuhn and E. Braun, *Naturwissenschaften*, 1929, **17**, 227–228; (*b*) W. Kuhn and E. Knopf, *Naturwissenschaften*, 1930, **18**, 183.
20 N. Demirel, P. Moths, X. Xie, S. I. Ivlev and E. Meggers, *Chemistry*, 2025, **31**, e202403792.
21 (*a*) J. B. Kidd, T. A. Fiala, W. B. Swords, Y. Park, K. A. Meyer, K. M. Sanders, I. A. Guzei, J. C. Wright and T. P. Yoon, *J. Am. Chem. Soc.*, 2024, **146**, 15293–15300; (*b*) W. B. Swords, H. Lee, Y. Park, F. Llamas, K. L. Skubi, J. Park, I. A. Guzei, M. H. Baik and T. P. Yoon, *J. Am. Chem. Soc.*, 2023, **145**, 27045–27053.
22 (*a*) R. Maeda, T. Wada, T. Mori, S. Kono, N. Kanomata and Y. Inoue, *J. Am. Chem. Soc.*, 2011, **133**, 10379–10381; (*b*) T. Bach, H. Bergmann and K. Harms, *Angew. Chem., Int. Ed.*, 2000, **39**, 2302–2304.
23 M. J. Genzink, J. B. Kidd, W. B. Swords and T. P. Yoon, *Chem. Rev.*, 2022, **122**, 1654–1716.
24 For selected reviews of visible-light/Ni dual catalysis: (*a*) H. Wang and T. Xu, *Chem. Catal.*, 2024, **4**, 100952; (*b*) U. Afzal, M. Bilal, M. Zubair, N. Rasool, S. Adnan Ali Shah and Z. Amiruddin Zakaria, *J. Saudi Chem. Soc.*, 2023, **27**, 101589; (*c*) X. Wu, P. Zheng, W. Li and T. Xu, *Org. Chem. Front.*, 2021, **8**, 4118–4123; (*d*) Z. D. Mou, J. X. Wang, X. Zhang and D. Niu, *Adv. Synth. Catal.*, 2021, **363**, 3025–3029; (*e*) W. Xu, P. Zheng and T. Xu, *Org. Lett.*, 2020, **22**, 8643–8647; (*f*) A. Dewanji, R. F. Bulow and M. Rueping, *Org. Lett.*, 2020, **22**, 1611–1617; (*g*) L. Peng, Z. Li and G. Yin, *Org. Lett.*, 2018, **20**, 1880–1883; (*h*) A. Paul, M. D. Smith and A. K. Vannucci, *J. Org. Chem.*, 2017, **82**, 1996–2003; (*i*) L. Yi, T. Ji, K.-Q. Chen, X.-Y. Chen and M. Rueping, *CCS Chem.*, 2022, **4**, 9–30.
25 For selected reviews of visible-light/Co dual catalysis: (*a*) S.-Q. Zhang, Y.-L. Li, K. Cui, C. Chen, Z.-Y. Gu, H. He and J.-B. Xia, *Org. Chem. Front.*, 2023, **10**, 6070–6080; (*b*) Z. Y. Gu, W. D. Li, Y. L. Li, K. Cui and J. B. Xia, *Angew. Chem., Int. Ed.*, 2023, **62**, e202213281; (*c*) W. D. Li, Y. Wu, S. J. Li, Y. Q. Jiang, Y. L. Li, Y. Lan and J. B. Xia, *J. Am. Chem. Soc.*, 2022, **144**, 8551–8559; (*d*) K. Ram Bajya and S. Selvakumar, *Eur. J. Org. Chem.*, 2022, e202200229.
26 For selected reviews of visible-light/Ru dual catalysis: R. Cao, Y. Liu, X. Shi and J. Zheng, *Chem. Commun.*, 2023, **59**, 10668–10671.
27 For selected reviews of visible-light/Ir dual catalysis: (*a*) P. J. Xia, Z. P. Ye, D. Song, J. W. Ren, H. W. Wu, J. A. Xiao, H. Y. Xiang, X. Q. Chen and H. Yang, *Chem. Commun.*, 2019, **55**, 2712–2715; (*b*) R. Wang, M. Ma, X. Gong, X. Fan and P. J. Walsh, *Org. Lett.*, 2019, **21**, 27–31; (*c*) M. Miao, L.-L. Liao, G.-M. Cao, W.-J. Zhou and D.-G. Yu, *Sci. China: Chem.*, 2019, **62**, 1519–1524; (*d*) Z. Liu, X. Nan, T. Lei, C. Zhou, Y. Wang, W. Liu, B. Chen, C. Tung and L. Wu, *Chin. J. Catal.*, 2018, **39**, 487–494.
28 For selected reviews of visible-light/Sm dual catalysis: T. Kuribara, A. Kaneki, Y. Matsuda and T. Nemoto, *J. Am. Chem. Soc.*, 2024, **146**, 20904–20912.
29 For selected reviews of visible-light/Sc dual catalysis: B. R. McDonald and K. A. Scheidt, *Org. Lett.*, 2018, **20**, 6877–6881.
30 For selected reviews of visible-light/metal-free catalysis: (*a*) Y. Xia, L. Sun, J. Cheng, S. Wang, M. Zheng and X. Wang, *Sci. China: Chem.*, 2024, **68**, 181–185; (*b*) W. Zhou, I. A. Dmitriev and P. Melchiorre, *J. Am. Chem. Soc.*, 2023, **145**, 25098–25102; (*c*) N. Tang, R. J. Zachmann, H. Xie, J. Zheng and B. Breit, *Chem. Commun.*, 2023, **59**, 2122–2125; (*d*) J. M. Yu, L. W. Zhu, X. Y. Hong, H. Gao and T. T. Chen, *Org. Biomol. Chem.*, 2021, **19**, 5642–5648; (*e*) X. Xu, Q. Q. Min, N. Li and F. Liu, *Chem. Commun.*, 2018, **54**, 11017–11020; (*f*) T. Sengoku, H. Iwama, T. Shimotori, K. Fujimoto, T. Inuzuka, K. Matsune and H. Yoda, *J. Org. Chem.*, 2023, **88**, 12776–12782.
31 (*a*) H.-H. Zhang, H. Chen, C. Zhu and S. Yu, *Sci. China Chem.*, 2020, **63**, 637–647; (*b*) J. Ma, X. Zhang, X. Huang, S. Luo and E. Meggers, *Nat. Protoc.*, 2018, **13**, 605–632; (*c*) J. Twilton, C. Le, P. Zhang, M. H. Shaw, R. W. Evans and D. W. C. MacMillan, *Nat. Rev. Chem.*, 2017, **1**, 0052; (*d*) K. P. S. Cheung, S. Sarkar and V. Gevorgyan, *Chem. Rev.*, 2022, **122**, 1543–1625; (*e*) M. Silvi and P. Melchiorre, *Nature*, 2018, **554**, 41–49; (*f*) Z. C. Litman, Y. Wang, H. Zhao and J. F. Hartwig, *Nature*, 2018, **560**, 355–359; (*g*) Z. Wang, Z. P. Yang and G. C. Fu, *Nat. Chem.*, 2021, **13**, 236–242; (*h*) H. Huo, B. J. Gorsline and G. C. Fu, *Science*, 2020, **367**, 559–564; (*i*) M. Guisan-Ceinos, V. Martin-Heras and M. Tortosa, *J. Am. Chem. Soc.*, 2017, **139**, 8448–8451; (*j*) J. Schmidt, J. Choi, A. T. Liu, M. Slusarczyk and G. C. Fu, *Science*, 2016, **354**, 1265–1269; (*k*) C. Fischer and G. C. Fu, *J. Am. Chem. Soc.*, 2005, **127**, 4594–4595; (*l*) X.-Y. Dong, Y.-F. Zhang, C.-L. Ma, Q.-S. Gu, F.-L. Wang, Z.-L. Li, S.-P. Jiang and X.-Y. Liu, *Nat. Chem.*, 2019, **11**, 1158–1166; (*m*) W.-T. Zhao and W. Shu, *Sci. Adv.*, 2023, **9**, 9898; (*n*) K. E. Poremba, S. E. Dibrell and S. E. Reisman, *ACS Catal.*, 2020, **10**, 8237–8246; (*o*) J. Choi and G. C. Fu, *Science*, 2017, **356**, 7230.
32 (*a*) X. Wang, Y. Dai and H. Gong, *Top. Curr. Chem.*, 2016, **374**, 43; (*b*) F. D. Lu, J. Chen, X. Jiang, J. R. Chen, L. Q. Lu and W. J. Xiao, *Chem. Soc. Rev.*, 2021, **50**, 12808–12827.
33 S. Z. Tasker, E. A. Standley and T. F. Jamison, *Nature*, 2014, **509**, 299–309.
34 (*a*) J. C. Tellis, C. B. Kelly, D. N. Primer, M. Jouffroy, N. R. Patel and G. A. Molander, *Acc. Chem. Res.*, 2016, **49**, 1429–1439; (*b*) M. Yuan and O. Gutierrez, *Wiley Interdiscip. Rev.: Comput. Mol. Sci.*, 2022, **12**, e1573.
35 (*a*) M. Yuan, Z. Song, S. O. Badir, G. A. Molander and O. Gutierrez, *J. Am. Chem. Soc.*, 2020, **142**, 7225–7234; (*b*) Q.-Y. Huang and M. Shi, *Org. Chem. Front.*, 2024, **11**, 4913–4925; (*c*) R. Wang, Y. Fang and C. Wang, *Cell Rep. Phys. Sci.*, 2024, **5**, 102216.
36 S. O. Badir and G. A. Molander, *Chem*, 2020, **6**, 1327–1339.

37 D. A. Everson and D. J. Weix, *J. Org. Chem.*, 2014, **79**, 4793–4798.
38 S. Biswas and D. J. Weix, *J. Am. Chem. Soc.*, 2013, **135**, 16192–16197.
39 D. J. Brauer and C. Krueger, *Inorg. Chem.*, 2002, **16**, 884–891.
40 Q. Ren, F. Jiang and H. Gong, *J. Organomet. Chem.*, 2014, **770**, 130–135.
41 G. S. Kumar, A. Peshkov, A. Brzozowska, P. Nikolaienko, C. Zhu and M. Rueping, *Angew. Chem., Int. Ed.*, 2020, **59**, 6513–6519.
42 (*a*) A. A. Isse, C. Y. Lin, M. L. Coote and A. Gennaro,, *J. Phys. Chem. B*, 2011, **115**, 678–684; (*b*) C. E. Knappke, S. Grupe, D. Gartner, M. Corpet, C. Gosmini and A. Jacobi von Wangelin, *Chemistry*, 2014, **20**, 6828–6842; (*c*) J. B. Diccianni and T. Diao, *Trends Chem.*, 2019, **1**, 830–844.
43 (*a*) D. A. Everson, B. A. Jones and D. J. Weix, *J. Am. Chem. Soc.*, 2012, **134**, 6146–6159; (*b*) X. Wang, S. Wang, W. Xue and H. Gong, *J. Am. Chem. Soc.*, 2015, **137**, 11562–11565; (*c*) T. B. Hamby, M. J. LaLama and C. S. Sevov, *Science*, 2022, **376**, 410–416.
44 (*a*) A. Wurtz, *Justus Liebigs Ann. Chem.*, 2006, **96**, 364–375; (*b*) B. Tollens and R. Fittig, *Justus Liebigs Ann. Chem.*, 2006, **131**, 303–323.
45 (*a*) Z. M. Su, R. Deng and S. S. Stahl, *Nat. Chem.*, 2024, **16**, 2036–2043; (*b*) L. E. Ehehalt, O. M. Beleh, I. C. Priest, J. M. Mouat, A. K. Olszewski, B. N. Ahern, A. R. Cruz, B. K. Chi, A. J. Castro, K. Kang, J. Wang and D. J. Weix, *Chem. Rev.*, 2024, **124**, 13397–13569; (*c*) J. D. Fang, X. Pang and X. Z. Shu, *J. Am. Chem. Soc.*, 2025, **147**, 28313–28321; (*d*) J. L. Hofstra, A. H. Cherney, C. M. Ordner and S. E. Reisman, *J. Am. Chem. Soc.*, 2018, **140**, 139–142; (*e*) K. E. Poremba, N. T. Kadunce, N. Suzuki, A. H. Cherney and S. E. Reisman, *J. Am. Chem. Soc.*, 2017, **139**, 5684–5687; (*f*) N. T. Kadunce and S. E. Reisman, *J. Am. Chem. Soc.*, 2015, **137**, 10480–10483.
46 (*a*) D. J. Charboneau, H. Huang, E. L. Barth, C. C. Germe, N. Hazari, B. Q. Mercado, M. R. Uehling and S. L. Zultanski, *J. Am. Chem. Soc.*, 2021, **143**, 21024–21036; (*b*) D. J. Charboneau, N. Hazari and H. Huang, *J. Org. Chem.*, 2022, **87**, 7589–7609.
47 P. Zhang, C. C. Le and D. W. MacMillan, *J. Am. Chem. Soc.*, 2016, **138**, 8084–8087.
48 Z. Duan, W. Li and A. Lei, *Org. Lett.*, 2016, **18**, 4012–4015.
49 H. Wang, P. Zheng, X. Wu, Y. Li and T. Xu, *J. Am. Chem. Soc.*, 2022, **144**, 3989–3997.
50 H. Guan, Q. Zhang, P. J. Walsh and J. Mao, *Angew. Chem., Int. Ed.*, 2020, **59**, 5172–5177.
51 H. Dhall, A. Kumar and A. K. Mishra, *Curr. Bioact. Compd.*, 2018, **14**, 26–32.
52 (*a*) Q. Lu, H. Guan, Y. E. Wang, D. Xiong, T. Lin, F. Xue and J. Mao, *J. Org. Chem.*, 2022, **87**, 8048–8058; (*b*) F. Xing, T. Lin, Y. Ye, Y. E. Wang, X. Cao, X. Gao, D. Zhang, L. Kong, X. Zhu, D. Xiong and J. Mao, *Chem. Commun.*, 2023, **59**, 13355–13358; (*c*) T. Li, X. Cheng, J. Lu, H. Wang, Q. Fang and Z. Lu, *Chin. J. Chem.*, 2022, **40**, 1033–1038.
53 P. Zheng, P. Zhou, D. Wang, W. Xu, H. Wang and T. Xu, *Nat. Commun.*, 2021, **12**, 1646.
54 P. Zhou, X. Li, D. Wang and T. Xu, *Org. Lett.*, 2021, **23**, 4683–4687.
55 S. Wen, J. Bu and K. Shen, *J. Org. Chem.*, 2024, **89**, 16134–16144.
56 J. G. Smith, *Synthesis*, 1984, 629–656.
57 E. N. Jacobsen, *Acc. Chem. Res.*, 2000, **33**, 421–431.
58 (*a*) I. Pastor and M. Yus, *Curr. Org. Chem.*, 2005, **9**, 1–29; (*b*) A. Lidskog, Y. Li and K. Wärnmark, *Catalysts*, 2020, **10**, 705.
59 N. Oguni, Y. Miyagi and K. Itoh, *Tetrahedron Lett.*, 1998, **39**, 9023–9026.
60 Y. Zhao and D. J. Weix, *J. Am. Chem. Soc.*, 2015, **137**, 3237–3240.
61 A. Banerjee and H. Yamamoto, *Org. Lett.*, 2017, **19**, 4363–4366.
62 S. H. Lau, M. A. Borden, T. J. Steiman, L. S. Wang, M. Parasram and A. G. Doyle, *J. Am. Chem. Soc.*, 2021, **143**, 15873–15881.
63 Z. Li, L. Huan, J. Li, X. Shu, D. Zhong, W. Zhang and H. Huo, *Angew. Chem., Int. Ed.*, 2023, **62**, e202305889.
64 (*a*) G. Laudadio, M. D. Palkowitz, T. El-Hayek Ewing and P. S. Baran, *ACS Med. Chem. Lett.*, 2022, **13**, 1413–1420; (*b*) A. W. Dombrowski, N. J. Gesmundo, A. L. Aguirre, K. A. Sarris, J. M. Young, A. R. Bogdan, M. C. Martin, S. Gedeon and Y. Wang, *ACS Med. Chem. Lett.*, 2020, **11**, 597–604; (*c*) C. N. Prieto Kullmer, J. A. Kautzky, S. W. Krska, T. Nowak, S. D. Dreher and D. W. C. MacMillan, *Science*, 2022, **376**, 532–539.
65 Z. Zuo, H. Cong, W. Li, J. Choi, G. C. Fu and D. W. MacMillan, *J. Am. Chem. Soc.*, 2016, **138**, 1832–1835.
66 D. J. Weix, *Acc. Chem. Res.*, 2015, **48**, 1767–1775.
67 B. A. Vara, N. R. Patel and G. A. Molander, *ACS Catal.*, 2017, **7**, 3955–3959.
68 (*a*) X. Cui, S. Wang, Y. Zhang, W. Deng, Q. Qian and H. Gong, *Org. Biomol. Chem.*, 2013, **11**, 3094–3097; (*b*) L. L. Anka-Lufford, M. R. Prinsell and D. J. Weix, *J. Org. Chem.*, 2012, **77**, 9989–10000.
69 (*a*) X. Tao, Y. Chen, J. Guo, X. Wang and H. Gong, *Chem. Sci.*, 2020, **12**, 220–226; (*b*) M. O. Konev, L. E. Hanna and E. R. Jarvo, *Angew. Chem., Int. Ed.*, 2016, **55**, 6730–6733.
70 L. K. G. Ackerman, L. L. Anka-Lufford, M. Naodovic and D. J. Weix, *Chem. Sci.*, 2015, **6**, 1115–1119.
71 (*a*) M. Gao, D. Sun and H. Gong, *Org. Lett.*, 2019, **21**, 1645–1648; (*b*) X. B. Yan, C. L. Li, W. J. Jin, P. Guo and X. Z. Shu, *Chem. Sci.*, 2018, **9**, 4529–4534; (*c*) X. Zhang and D. W. C. MacMillan, *J. Am. Chem. Soc.*, 2016, **138**, 13862–13865.
72 Y. Pan, Y. Gong, Y. Song, W. Tong and H. Gong, *Org. Biomol. Chem.*, 2019, **17**, 4230–4233.
73 (*a*) K. Komeyama, R. Ohata, S. Kiguchi and I. Osaka, *Chem. Commun.*, 2017, **53**, 6401–6404; (*b*) J. Wang, J. Zhao and H. Gong, *Chem. Commun.*, 2017, **53**, 10180–10183; (*c*) G. A. Molander, K. M. Traister and B. T. O'Neill, *J. Org. Chem.*, 2015, **80**, 2907–2911.

74 K. M. Arendt and A. G. Doyle, *Angew. Chem., Int. Ed.*, 2015, **54**, 9876–9880.
75 (*a*) M. Parasram, B. J. Shields, O. Ahmad, T. Knauber and A. G. Doyle, *ACS Catal.*, 2020, **10**, 5821–5827; (*b*) S. K. Kariofillis, S. Jiang, A. M. Zuranski, S. S. Gandhi, J. I. Martinez Alvarado and A. G. Doyle, *J. Am. Chem. Soc.*, 2022, **144**, 1045–1055; (*c*) S. K. Kariofillis, B. J. Shields, M. A. Tekle-Smith, M. J. Zacuto and A. G. Doyle, *J. Am. Chem. Soc.*, 2020, **142**, 7683–7689.
76 (*a*) Q. Lin, W. Tong, X. Z. Shu and Y. Chen, *Org. Lett.*, 2022, **24**, 8459–8464; (*b*) T. Suga, Y. Takahashi, C. Miki and Y. Ukaji, *Angew. Chem., Int. Ed.*, 2022, **61**, e202112533; (*c*) H. Xie, S. Wang, Y. Wang, P. Guo and X.-Z. Shu, *ACS Catal.*, 2022, **12**, 1018–1023; (*d*) T. Suga, S. Shimazu and Y. Ukaji, *Org. Lett.*, 2018, **20**, 5389–5392; (*e*) T. Suga, Y. Takahashi and Y. Ukaji, *Adv. Synth. Catal.*, 2020, **362**, 5622–5626; (*f*) T. Suga and Y. Ukaji, *Org. Lett.*, 2018, **20**, 7846–7850.
77 Q. Lin, G. Ma and H. Gong, *ACS Catal.*, 2021, **11**, 14102–14109.
78 (*a*) P. Guo, K. Wang, W. J. Jin, H. Xie, L. Qi, X. Y. Liu and X. Z. Shu, *J. Am. Chem. Soc.*, 2021, **143**, 513–523; (*b*) F.-F. Pan, P. Guo, X. Huang and X.-Z. Shu, *Synthesis*, 2021, 3094–3100.
79 B. K. Chi, J. K. Widness, M. M. Gilbert, D. C. Salgueiro, K. J. Garcia and D. J. Weix, *ACS Catal.*, 2022, **12**, 580–586.
80 (*a*) Y. Li, Z. Wang, L. Li, X. Tian, F. Shao and C. Li, *Angew. Chem., Int. Ed.*, 2022, **61**, e202110391; (*b*) Z. Li, W. Sun, X. Wang, L. Li, Y. Zhang and C. Li, *J. Am. Chem. Soc.*, 2021, **143**, 3536–3543.
81 (*a*) Z. Fan, S. Chen, S. Zou and C. Xi, *ACS Catal.*, 2022, **12**, 2781–2787; (*b*) M. van Gemmeren, M. Borjesson, A. Tortajada, S. Z. Sun, K. Okura and R. Martin, *Angew. Chem., Int. Ed.*, 2017, **56**, 6558–6562.
82 (*a*) Z. Dong and D. W. C. MacMillan, *Nature*, 2021, **598**, 451–456; (*b*) C. A. Gould, A. L. Pace and D. W. C. MacMillan, *J. Am. Chem. Soc.*, 2023, **145**, 16330–16336; (*c*) W. L. Lyon and D. W. C. MacMillan, *J. Am. Chem. Soc.*, 2023, **145**, 7736–7742.
83 L. L. Zhang, Y. Z. Gao, S. H. Cai, H. Yu, S. J. Shen, Q. Ping and Z. P. Yang, *Nat. Commun.*, 2024, **15**, 2733.
84 G. Xu, C. H. Senanayake and W. Tang, *Acc. Chem. Res.*, 2019, **52**, 1101–1112.
85 H. Wang, X. Wu and T. Xu, *Angew. Chem., Int. Ed.*, 2023, **62**, e202218299.
86 (*a*) K. Müller, C. Faeh and F. O. Diederich, *Science*, 2007, **317**, 1881–1886; (*b*) J. Wang, M. Sánchez-Roselló, J. L. Aceña, C. del Pozo, A. E. Sorochinsky, S. Fustero, V. A. Soloshonok and H. Liu, *Chem. Rev.*, 2013, **114**, 2432–2506.
87 S. Lu, Z. Hu, D. Wang and T. Xu, *Angew. Chem., Int. Ed.*, 2024, **136**, e202406064.
88 J. Zhou, D. Wang, W. Xu, Z. Hu and T. Xu, *J. Am. Chem. Soc.*, 2023, **145**, 2081–2087.
89 P. Qian, H. Guan, Y. E. Wang, Q. Lu, F. Zhang, D. Xiong, P. J. Walsh and J. Mao, *Nat. Commun.*, 2021, **12**, 6613.
90 X. Li, Y. Hu, Z. Huang, S. Zhu, F.-L. Qing and L. Chu, *ACS Catal.*, 2024, **14**, 15790–15798.
91 S. Chakrabortty, B. de Bruin and J. G. de Vries, *Angew. Chem., Int. Ed.*, 2024, **136**, e202315773.
92 (*a*) S. Hassan, M. Bilal, S. Khalid, N. Rasool, M. Imran and A. A. Shah, *Mol. Divers.*, 2024, 1–50; (*b*) B. He, Q. Pan, Y. Guo, Q.-Y. Chen and C. Liu, *Org. Lett.*, 2020, **22**, 6552–6556; (*c*) H. Dong, Z. Lin and C. Wang, *Adv. Synth. Catal.*, 2023, **365**, 1165–1169; (*d*) S. Pal, S. Chowdhury, E. Rozwadowski, A. Auffrant and C. Gosmini, *Adv. Synth. Catal.*, 2016, **358**, 2431–2435; (*e*) X. Zhang, J. Wang and S.-D. Yang, *ACS Catal.*, 2021, **11**, 14008–14015; (*f*) W.-Y. Ma, G.-Y. Han, S. Kang, X. Pang, X.-Y. Liu and X.-Z. Shu, *J. Am. Chem. Soc.*, 2021, **143**, 15930–15935.
93 M. Kojima and S. Matsunaga, *Trends Chem.*, 2020, **2**, 410–426.
94 Y. Li, X. Lu and Y. Fu, *CCS Chem.*, 2024, **6**, 1130–1156.
95 (*a*) E. Skucas, M. Y. Ngai, V. Komanduri and M. J. Krische, *Acc. Chem. Res.*, 2007, **40**, 1394–1401; (*b*) M. Holmes, L. A. Schwartz and M. J. Krische, *Chem. Rev.*, 2018, **118**, 6026–6052; (*c*) R. Y. Liu and S. L. Buchwald, *Acc. Chem. Res.*, 2020, **53**, 1229–1243.
96 (*a*) R. M. Moslin, K. Miller-Moslin and T. F. Jamison, *Chem. Commun.*, 2007, 4441–4449; (*b*) M. Jeganmohan and C. H. Cheng, *Chemistry*, 2008, **14**, 10876–10886.
97 Y.-L. Li, S.-Q. Zhang, J. Chen and J.-B. Xia, *J. Am. Chem. Soc.*, 2021, **143**, 7306–7313.
98 T. Liang, Y. Wu, J. Sun, M. Li, H. Zhao, J. Zhang, G. Zheng and Q. Zhang, *Chin. J. Chem.*, 2023, **41**, 3253–3260.
99 (*a*) C.-C. Wang, P.-S. Lin and C.-H. Cheng, *Tetrahedron Lett.*, 2004, **45**, 6203–6206; (*b*) S. M. Weber and G. Hilt, *Front. Chem.*, 2021, **9**, 635826.
100 C. H. Wei, S. Mannathan and C. H. Cheng, *J. Am. Chem. Soc.*, 2011, **133**, 6942–6944.
101 K. Cui, Y. L. Li, G. Li and J. B. Xia, *J. Am. Chem. Soc.*, 2022, **144**, 23001–23009.
102 T. Zeng, Y. He, Y. Li, L. Wang, Q. Hu, Y. Li, Z. Wei, J. Chen, X. Qi and J. Zhu, *Nat. Commun.*, 2025, **16**, 3102.
103 B. Dongya, H. Junyao, O. Bin, H. Jin and W. Pu, *Prog. Chem.*, 2017, **29**, 491–501.
104 K. Yabushita, A. Yuasa, K. Nagao and H. Ohmiya, *J. Am. Chem. Soc.*, 2019, **141**, 113–117.
105 X. Jiang, H. Jiang, Q. Yang, Y. Cheng, L. Q. Lu, J. A. Tunge and W. J. Xiao, *J. Am. Chem. Soc.*, 2022, **144**, 8347–8354.
106 H. Jiang, X. K. He, X. Jiang, W. Zhao, L. Q. Lu, Y. Cheng and W. J. Xiao, *J. Am. Chem. Soc.*, 2023, **145**, 6944–6952.
107 T. Han, Q. Mou, Y. Lv and M. Liu, *Green Chem.*, 2024, **26**, 1370–1374.
108 X. Jiang, W. Xiong, S. Deng, F.-D. Lu, Y. Jia, Q. Yang, L.-Y. Xue, X. Qi, J. A. Tunge, L.-Q. Lu and W.-J. Xiao, *Nat. Catal.*, 2022, **5**, 788–797.
109 (*a*) F. Zhou, X. Hu, W. Zhang and C.-J. Li, *Org. Chem. Front.*, 2018, **5**, 3579–3584; (*b*) R. Shrestha, S. C. Dorn and D. J. Weix, *J. Am. Chem. Soc.*, 2013, **135**, 751–762.
110 (*a*) G. Yue, K. Lei, H. Hirao and J. S. Zhou, *Angew. Chem., Int. Ed.*, 2015, **54**, 6531–6535; (*b*) S. Mannathan,

S. Raoufmoghaddam, J. N. H. Reek, J. G. de Vries and A. J. Minnaard, *ChemCatChem*, 2017, **9**, 551–554.
111 X. Qin, M. W. Yao Lee and J. S. Zhou, *Org. Lett.*, 2019, **21**, 5990–5994.
112 L. Zhang, M. Zhao, M. Pu, Z. Ma, J. Zhou, C. Chen, Y. D. Wu, Y. R. Chi and J. S. Zhou, *J. Am. Chem. Soc.*, 2022, **144**, 20249–20257.
113 W. Xiong, X. Jiang, W. C. Wang, Y. Cheng, L. Q. Lu, K. Gao and W. J. Xiao, *J. Am. Chem. Soc.*, 2023, **145**, 7983–7991.
114 E. A. Standley, S. Z. Tasker, K. L. Jensen and T. F. Jamison, *Acc. Chem. Res.*, 2015, **48**, 1503–1514.
115 M. Maiti, S. K. Jana and B. Maji, *Chem. Commun.*, 2023, **59**, 9718–9721.
116 (*a*) J. W. B. Fyfe and A. J. B. Watson, *Chem*, 2017, **3**, 31–55; (*b*) D. M. Volochnyuk, A. O. Gorlova and O. O. Grygorenko, *Chemistry*, 2021, **27**, 15277–15326.
117 Z. Chi, J. B. Liao, X. Cheng, Z. Ye, W. Yuan, Y. M. Lin and L. Gong, *J. Am. Chem. Soc.*, 2024, **146**, 10857–10867.
118 Q. Liu, X. Dong, J. Li, J. Xiao, Y. Dong and H. Liu, *ACS Catal.*, 2015, **5**, 6111–6137.
119 O. Pamies, J. Margalef, S. Canellas, J. James, E. Judge, P. J. Guiry, C. Moberg, J. E. Backvall, A. Pfaltz, M. A. Pericas and M. Dieguez, *Chem. Rev.*, 2021, **121**, 4373–4505.
120 H. H. Zhang, M. Tang, J. J. Zhao, C. Song and S. Yu, *J. Am. Chem. Soc.*, 2021, **143**, 12836–12846.
121 S. Tang, H. H. Zhang and S. Yu, *Chem. Commun.*, 2023, **59**, 1153–1156.
122 X. Wu, Y. Chang and S. Lin, *Chem*, 2022, **8**, 1805–1821.
123 (*a*) A. Bongso, R. Roswanda and Y. M. Syah, *RSC Adv.*, 2022, **12**, 15885–15909; (*b*) A. Chatterjee, T. H. Bennur and N. N. Joshi, *J. Org. Chem.*, 2003, **68**, 5668–5671.
124 F. Calogero, G. Magagnano, S. Potenti, F. Pasca, A. Fermi, A. Gualandi, P. Ceroni, G. Bergamini and P. G. Cozzi, *Chem. Sci.*, 2022, **13**, 5973–5981.
125 (*a*) M. J. Genzink, J. B. Kidd, W. B. Swords and T. P. Yoon, *Chem. Rev.*, 2022, **122**, 1654–1716; (*b*) X. Huang and E. Meggers, *Acc. Chem. Res.*, 2019, **52**, 833–847.
126 P. Dey, P. Rai and B. Maji, *ACS Org. Inorg. Au*, 2022, **2**, 99–125.
127 X. Huang, S. Luo, O. Burghaus, R. D. Webster, K. Harms and E. Meggers, *Chem. Sci.*, 2017, **8**, 7126–7131.
128 J. Ma, J. Lin, L. Zhao, K. Harms, M. Marsch, X. Xie and E. Meggers, *Angew. Chem., Int. Ed.*, 2018, **57**, 11193–11197.
129 F. H. Arnold, *Angew. Chem., Int. Ed.*, 2018, **57**, 4143–4148.
130 P. D. Clayman and T. K. Hyster, *J. Am. Chem. Soc.*, 2020, **142**, 15673–15677.
131 H. Fu, J. Cao, T. Qiao, Y. Qi, S. J. Charnock, S. Garfinkle and T. K. Hyster, *Nature*, 2022, **610**, 302–307.
132 D. Parmar, E. Sugiono, S. Raja and M. Rueping, *Chem. Rev.*, 2014, **114**, 9047–9153.
133 L. J. Rono, H. G. Yayla, D. Y. Wang, M. F. Armstrong and R. R. Knowles, *J. Am. Chem. Soc.*, 2013, **135**, 17735–17738.
134 (*a*) A. Y. Guan, C. L. Liu, X. F. Sun, Y. Xie and M. A. Wang, *Bioorg. Med. Chem.*, 2016, **24**, 342–353; (*b*) G. Chelucci, *Coord. Chem. Rev.*, 2013, **257**, 1887–1932.
135 K. Cao, S. M. Tan, R. Lee, S. Yang, H. Jia, X. Zhao, B. Qiao and Z. Jiang, *J. Am. Chem. Soc.*, 2019, **141**, 5437–5443.
136 M. Kong, Y. Tan, X. Zhao, B. Qiao, C. H. Tan, S. Cao and Z. Jiang, *J. Am. Chem. Soc.*, 2021, **143**, 4024–4031.

